

Hybrid Provision of Energy based on Reliability and Resiliency by Integration of Dc Equipment

Work Package WP3

Laboratory validation services for DC components & systems (LV and MV)

Deliverable D3.4

Test and Validation Procedures and Services

Funding Instrument: Innovation Action
Call: H2020-LC-SC3-2020-EC-ES-SCC
Call Topic: LC-SC3-ES-10-2020 - DC – AC/DC hybrid grid for a modular, resilient and high RES share grid development

Project Start: 1 October 2020
Project Duration: 48 months

Beneficiary in Charge: AIT Austrian Institute of Technology GmbH

Document Identifier: doi:[10.5281/zenodo.6102453](https://doi.org/10.5281/zenodo.6102453)

Dissemination Level		
PU	Public	✓
PP	Restricted to other programme participants (including the Commission Services)	
RE	Restricted to a group specified by the Consortium (including the Commission Services)	
CO	Confidential, only for members of the Consortium (including the Commission Services)	



Deliverable Information

Document Administrative Information	
Project Acronym:	HYPERRIDE
Project Number:	957788
Deliverable Number:	D3.4
Deliverable Full Title:	Test and Validation Procedures and Services
Deliverable Short Title:	Test and Validation Procedures and Services
Document Identifier:	HYPERRIDE-D34-TestAndValidationProceduresAndServices-submitted
Beneficiary in Charge:	AIT Austrian Institute of Technology GmbH
Report Version:	v1.3
Contractual Date:	31/10/2020
Report Submission Date:	02/12/2024
Dissemination Level:	PU
Nature:	Report
Lead Author(s):	Marcus Milnera, G. Lauss (AIT)
Co-author(s):	Gerhard Jambrich (AIT), Bence Hátsági (Scibreak AB), Simon Nee (Scibreak AB), Johannes Böhm (Zelisko), Francesco Bellesini (EMOT), Michael Holzbauer (Zelisko), Jan Mathé (RWTH Aachen), Tim Karsten (RWTH Aachen), Katharina Hetzenecker (RWTH Aachen), S. Costea (Eaton), D. Dujic (EPFL), M. Cresta (ASM Terni Spa)
Keywords:	DC systems, LVDC, MVDC, HVDC, DC/AC grids, testing methods, DC-arc, standardisation, validation, European Union (EU), H2020, Project, HYPER-RIDE, GA 957788
Status:	<input type="checkbox"/> draft, <input type="checkbox"/> final, <input checked="" type="checkbox"/> submitted

Change Log

Date	Version	Author/Editor	Summary of Changes Made
10/03/2020	V1.0	M. Milnera (AIT)	Initial document structure, section inputs and draft for review
25/07/2022	V1.1	G. Lauss (AIT)	Extended description of DC related laboratory testing facilities
04/10/2024	V1.2	G. Lauss, M. Milnera (AIT)	Editing and finalising all Subsections for the final Deliverable
02/12/2024	V1.3	G. Jambrich (AIT)	Final version

Table of Contents

Executive Summary	8
1. Introduction	9
1.1 Purpose and Scope of the Document	9
1.2 Structure of the Document	9
2. Test Infrastructure of HYPERRIDE-Partners	10
2.1 AIT	10
2.2 SCIBREAK	19
2.3 EATON	21
2.4 RWTH Aachen	23
2.5 EPFL	24
2.6 ZELISKO	26
2.7 EMOT	29
2.8 ASM Terni	38
3. Requirements on Test and Validation Services for HYPERRIDE and general DC- and AC/DC Grids	43
3.1 Fraunhofer IISB, Germany	44
3.2 Center of Advanced Power Systems (CAPS), Tallahassee, U.S.	46
3.3 Hydro-Québec's research institute (IREQ), Varennes, Canada	48
3.4 Existing Standards and Normative Frameworks	50
4. DC-Arc Fault Testing	54
5. Conclusions	57
References	58

List of Figures

Figure 1: Main components of the old test circuit.	10
Figure 2: New DC testing facility; Serial wiring of transformers for realisation of high voltages.	11
Figure 3: New DC testing facility; Parallel wiring of transformers for realisation of high currents.	11
Figure 4: 3-D CAD caption of the MVDC component test infrastructure at AIT.	12
Figure 5: Photographic illustration of the MVDC component test infrastructure at AIT in the building phase showing the high amount of installed copper.	13
Figure 6: Photographic illustration of the finalised MVDC component test infrastructure at AIT.	13
Figure 7: AIT SmartEST laboratory.	14
Figure 8: LVDC grid testbed.	15
Figure 9: Schematic test setup for active front end validation.	16
Figure 10: Laboratory setup with two AIT smart grid converters in a back-to-back setup.	17
Figure 11: C-HIL setup with two Typhoon HIL 602+ emulators and two AIT HIL controllers.	18
Figure 12: Simulation model for active front end validation	18
Figure 13: Test circuit connection.	19
Figure 14: Test circuit.	20
Figure 15: Eaton DC power systems laboratory.	21
Figure 16: Controller Hardware-in-the-Loop (CHIL) setup.	21
Figure 17: LTSpice schematics of the circuit used for TCA opening tests.	22
Figure 18: Testing setup for functional verification of the TCA prototype.	22
Figure 19: Overview of the hybrid MV/LV AC/DC microgrid.	23
Figure 20: Overview of the different control functionalities of the converters.	23
Figure 21: Scheme of EPFL demonstration site.	25
Figure 22: Equipment for converter commissioning.	25
Figure 23: Converters to be commissioned.	25
Figure 24: PD-measurement setup.	26
Figure 25: Current measuring bridge.	26
Figure 26: Temperature compensation setup (left); Hall sensor in the environmental test chamber (right).	27
Figure 27: Schematic of the experimental setup for mechanical force measurements.	28
Figure 28: DC accuracy measurement setup.	28
Figure 29: Zekalabs RedPrime DC/DC converter 40 kW, 750 V lab testing.	29
Figure 30: DC/DC converter registers reading.	30
Figure 31: DC/DC converter contactors block.	31
Figure 32: DC/DC converter connected to contactors block and AC/DC converter for lab testing.	32
Figure 33: AC/DC converter for lab testing.	33
Figure 34: DC/DC charging station cabinet.	34
Figure 35: DC/DC charging station cabinet forced air ventilation.	35
Figure 36: DC/DC charging station EVI.	36
Figure 37: DC/DC charging station converter installed in the cabinet.	37
Figure 38: Italian pilot - electric diagram.	38
Figure 39: Italian pilot - photovoltaic power plant.	39
Figure 40: Italian pilot - active front end converters.	39
Figure 41: Italian pilot - storage and photovoltaic DC power supply.	40
Figure 42: Italian pilot - second life cycle batteries.	41
Figure 43: Italian pilot - DC grid local control.	42
Figure 44: AC voltage level (in V) and the percentage (in %) of labs (source: JRC).	43
Figure 45: DC voltage level (in V) and the percentage (in %) of labs (source: JRC).	43
Figure 46: IISB MMC test facility (source: Fraunhofer IISB).	44

Figure 47: Medium voltage test bench at IISB (source: Fraunhofer IISB).	44
Figure 48: IISB supply connections (source: Fraunhofer IISB).....	45
Figure 49: IISB setups (source: Fraunhofer IISB).	46
Figure 50: HIL facility overview at CAPS (source: CAPS).....	47
Figure 51: Reconfigurable MW-class PHIL amplifier (source: CAPS).....	47
Figure 52: Real-time power system simulator lab at IREQ (source: Hydro-Québec).....	49
Figure 53: Full-scale distribution test line test setup at IREQ (source: Hydro-Québec).	49
Figure 54: SIMP power simulator at IREQ (source: Hydro-Québec).	50
Figure 55: (a) Enclosure used for DC-arc-testings (b) adjustable gap between busbars incl. igni- tion wire.	54
Figure 56: DC-arcing in the enclosure (without dark filter).	55
Figure 57: Time-Sequence using a dark optical filter showing the movement of the arc from left to right.	55
Figure 58: Oscillograph curves of current, voltage, pressure (p9), pressure (p10) and power (P).	56

List of Tables

Table 1: Summary of maximal values applicable for the test facility at AIT.	10
Table 2: Voltage, current, power, and impulse voltage ratings for LV/MV high current laboratory.	12
Table 3: Functional specification for HIL laboratory test for hybrid grid components (LV).....	15
Table 4: Values of the DC line impedances.	16
Table 5: Charged capacitor test circuit.	19
Table 6: Technical specifications of the Zekalabs RedPrime DC/DC converter.	30
Table 7: Technical specifications of the Zekalabs LB-1111-01 contactors block.	31
Table 8: Technical specifications of the SETEC POWER SDC450 AC/DC converter.....	33
Table 9: Relevant set of required LVDC component and system solutions.	51
Table 10: Relevant set of required MVDC component and system solutions.	51
Table 11: Overview over DC components and DC systems testing.	52
Table 12: Available LVDC standards	53

List of Abbreviations

AC	Alternating Current
AFE	Active Front End
ASGC	AIT Smart Grid Converter
BESS	Battery Energy Storage System
CHIL	Controller Hardware-in-the-Loop
DAB	Dual Active Bridge
DER	Distributed Energy Resource
DC	Direct Current
DC VVS	Direct Current Variable Voltage Source
DUT	Device under Test
FPGA	Field Programmable Gate Array
HIL	Hardware-in-the-Loop
HVDC	High Voltage Direct Current
IGBT	Insulated Gate Bipolar Transistor
LV	Low Voltage
LVDC	Low Voltage Direct Current
MMC	Multi Modular Converter
MV	Medium Voltage
MVDC	Medium Voltage Direct Current
PE	Power Electronics
PHIL	Power Hardware-in-the-Loop
PV	Photovoltaic
SCADA	Supervisory Control and Data Acquisition
SMU	Synchronised Measurement Unit
STATCOM	Static Synchronous Compensator
PEL	Power Electronics Laboratory
TCA	Thomson Coil Actuator
TO	Test Object
V2G	Vehicle to Grid

Executive Summary

New technologies as needed for the realization of DC grids need to be tested in an early stage of development and early adoption but also need to be tested with respect to standards and grid code compliance for certification. Within this task test and validation procedures will be proposed and implemented to enable such test and validation services. Potential applications will be novel, fast power electronic based DC circuit breakers and power converters for MVDC and LVDC as well as automation implementations via real-time simulation interfaces used in hardware-in-the-loop methods.

This document gives an overview on the HYPERRIDE-relevant test equipment and test procedures available at the partners sides and some other relevant sides. In what follows, a breakdown of LVDC, MVDC, and HVDC topics is used to summarise findings and requirements for this Deliverable.

In case of LVDC research and testing facilities, several well-equipped laboratory setups are already existing among HYPERRIDE partners, as can be seen in descriptions in Section 2. However, more advanced and more complex testing infrastructure is necessary to cover urgent needs for matching the demand of industry and for meeting the requirements necessary to ingrate DC system and components into existing grids.

For low MVDC topics, several facilities show distinct laboratory setups and well-equipped infrastructure for appropriate testing. The Fraunhofer IISB and the Center of Advanced Power Systems (CAPS) both have flexible test benches and supply connections in order to execute MVDC tests in the MW-range, as shown in Sections 3.1 and 3.2. Reconfigurable and high bandwidth amplification units provide the possibility to link the hardware setup for conduct real-time based HIL testing.

In case of HVDC applications, the research facility of Hydro Quebec shows the ability to conduct laboratory testing. As described in Section 3.3, a full-scale distribution test line test setup and a flexible real-time setup for HIL testing has been developed. Similar or comparable building blocks for higher MVDC testing are still missing at HYPERRIDE partners. For this purpose, the project "DC Hub Austria" has been recently initiated in order to assess planning and installing testing infrastructure for testing DC grids rated up to 60 kV combined with large-scale power (MW-class).

Based on findings in the HYPERRIDE project, it has to be summed up that large-scale pilot projects are missing on a European level. This goes along with a lack of cost-effective use-cases, lower technical readiness levels as well as insufficient normative frameworks which are not or not well applicable for the integration of DC applications in existing AC- or hybrid AC/DC distribution grids. This is valid for in particular for MVDC application, in which appropriate system requirements for high DC voltage (insulation level) combined with high power levels are necessary. Partly, these standards or guidelines have not been developed yet. For some DC applications, recommendations and guidelines for DC grid implementations could be identified (Jambrich & Fuchs, 2021) and other activities are still ongoing (CIRED WG 2021-1 "DC and hybrid DC/AC distribution networks integration").

In general, the harmonisation of existing normative frameworks or technical guidelines shows increased importance. Combined efforts are done to harmonise different system concepts for DC industry components and systems on an IEC level. For this purpose, networks and collaborations with international research and industrial partners are essential and first steps are already initiated (CIRED and CIGRE WGs with final reports and technical brochures).

1 Introduction

1.1 Purpose and Scope of the Document

The aim of Deliverable D3.4 is to give an overview about the testing facilities, testing accreditation, etc. of all HYPERRIDE-partners relevant to the goals of HYPERRIDE. It has to be noted that the task T3.4 is not finished by this delivery D3.4. The physical testings will be performed on demand during the whole duration of HYPERRIDE.

1.2 Structure of the Document

This work document is organised as follows:

- Section 1 provides information about the report content.
- Section 2 describes the testing facilities relevant for AC- and DC-testing of all HYPERRIDE-partners (AIT, SCIBREAK, EATON, RWTH Aachen, EPFL, ZELISKO, EMOT, and ASM Terni).
- Section 3 provides descriptions on requirements on test and validation services for HYPERRIDE and general DC- and AC/DC grids. Here, descriptions related to research facilities such as Fraunhofer IISB, Germany, the Center of Advanced Power Systems (CAPS), U.S, or the Hydro-Québec's research institute (IREQ), Canada are highlighted.
- Section 4 presents technical information on DC arc fault testing.
- Section 5 concludes this work and gives an outlook on future works.

2 Test Infrastructure of HYPERRIDE-Partners

This section gives an overview about the test infrastructure available at the HYPERRIDE-partners and relevant for the aims of HYPERRIDE.

2.1 AIT

Table 1 gives a summary of maximal values for Alternating Current (AC) and Direct Current (DC) test setups achievable at AIT. Especially the values for the new facility can differ strongly in both directions, larger or smaller.

Table 1: Summary of maximal values applicable for the test facility at AIT.

High Current AC	3 s	0.1 - 40 V	120 MW	150 kA
High Current DC	0.5 s	1 kV	75 MW	30 kA
High Voltage AC		600 kV		1 A
Impulse Voltage	LI	1.2 MV		
New High Current DC	0.5 s	(820; 1580; 3800) V	160 MVA	(20;40;80) kA

2.1.1 Old DC Testing Facility

The neck of the old DC testing facility is shown in Figure 1 and consists of an R6 rectifier which limits the current to 30 kA and approximately 0.5 ms duration due to thermal stress.

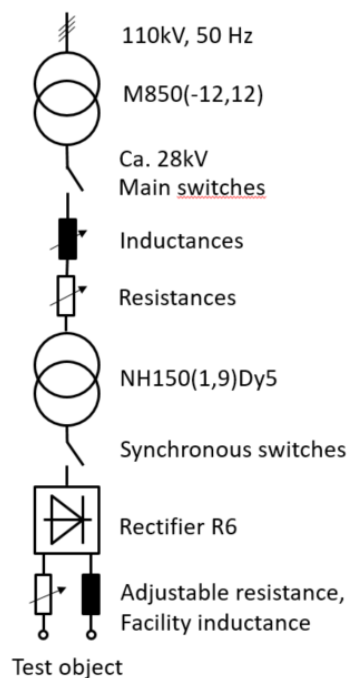


Figure 1: Main components of the old test circuit.

2.1.2 New DC Testing Facility

The new DC testing facility is realised by four transformers, which can be wired in different configurations. The transformers are equipped with three additional 30°-phase-shifted outputs. Figure 2 and Figure 3 show two different realisations of respective serial and parallel transformer wiring implemented in the laboratory infrastructure and with following technical settings:

- ISO-level 7,2 kV / 60 kV / 200 kV LI; short circuit power approx. 160 MVA; maximum short-circuit duration: 3 s.
- Short-circuit currents and initial voltages: 80 kA(@820 V); 40 kA(@1580 V); 20 kA(@3200 V).
- Permanent power 4 MVA (e.g. thermal withstand tests): 5,00 kA(@820 V); 2,50 kA(@1580 V); 1,25 kA(@3200 V).

Schaltungsvariante: Transformatoren oberspannungsseitig parallel, alle B6-Gleichrichter in Serie

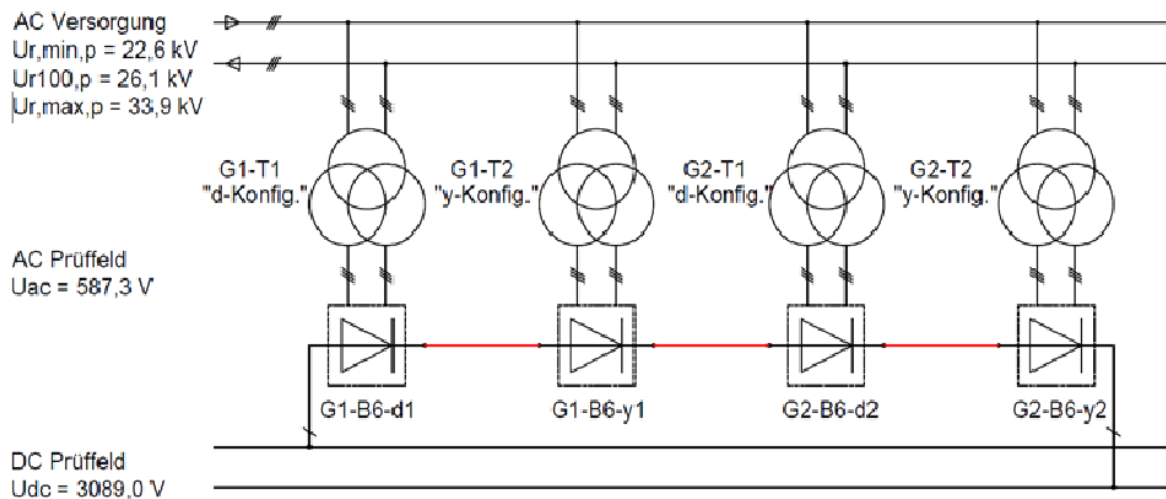


Figure 2: New DC testing facility; Serial wiring of transformers for realisation of high voltages.

Schaltungsvariante: Transformatoren oberspannungsseitig paarweise in Serie, alle Gleichrichter parallel

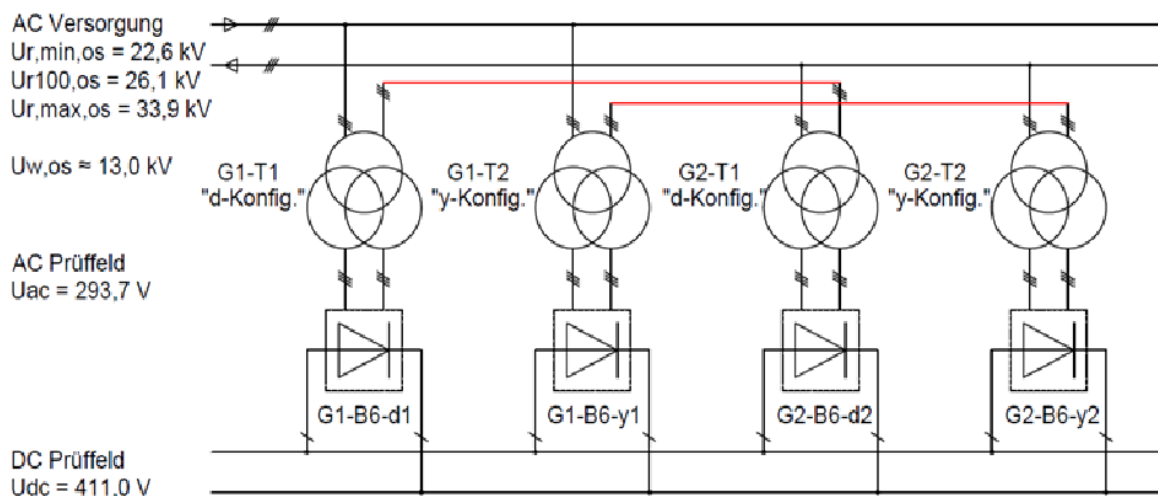


Figure 3: New DC testing facility; Parallel wiring of transformers for realisation of high currents.

MVDC and LVDC applications need to be tested according to given standards and existent regulations as a mandatory requirement for market introduction. A normative environment enables users to use validated products for reliable infrastructure installation. Advanced laboratory facilities are required supporting new concepts such as DC, Medium Voltage (MV), and Low Voltage (LV) grids in order to lever on existing AC test infrastructures. AIT permanently improves and upgrades its infrastructure capabilities focused on short circuit testing of DC components. For this purpose, a test facility involving configurable transformer and rectifier setups with high short circuit currents up to 80 kA has been implemented.

For the project HYPERRIDE it is intended to utilise this novel laboratory setup for the test case development of newly defined standards. Moreover, industry partners can be offered an enlarged test range applicable for accredited testing. Table 2 provides technical specification of the LV / MV high current laboratory.

Table 2: Voltage, current, power, and impulse voltage ratings for LV/MV high current laboratory.

Parameter	Values	Unit	Parameter	Values	Unit	Parameter	Values	Unit
High Current AC			High Current DC			High Voltage		
Voltage (3 s max)	0.1 - 40	kV	Voltage (100 ms)	0.1 - 3.8	kV	Voltage	600	kV
Power (3 s max)	120	MVA	Power (100 ms)	160	MW	Current	1	A
Current (3 s max)	150	kA	Current (100 ms)	80	kA	Voltage	600	kV
			Permanent power	4	MW	Impulse	1.2	MV

In Figure 4, a 3-D CAD caption of the MVDC test infrastructure at AIT is shown. In Figure 5 and Figure 6, photographic illustrations of the MVDC laboratory are provided.

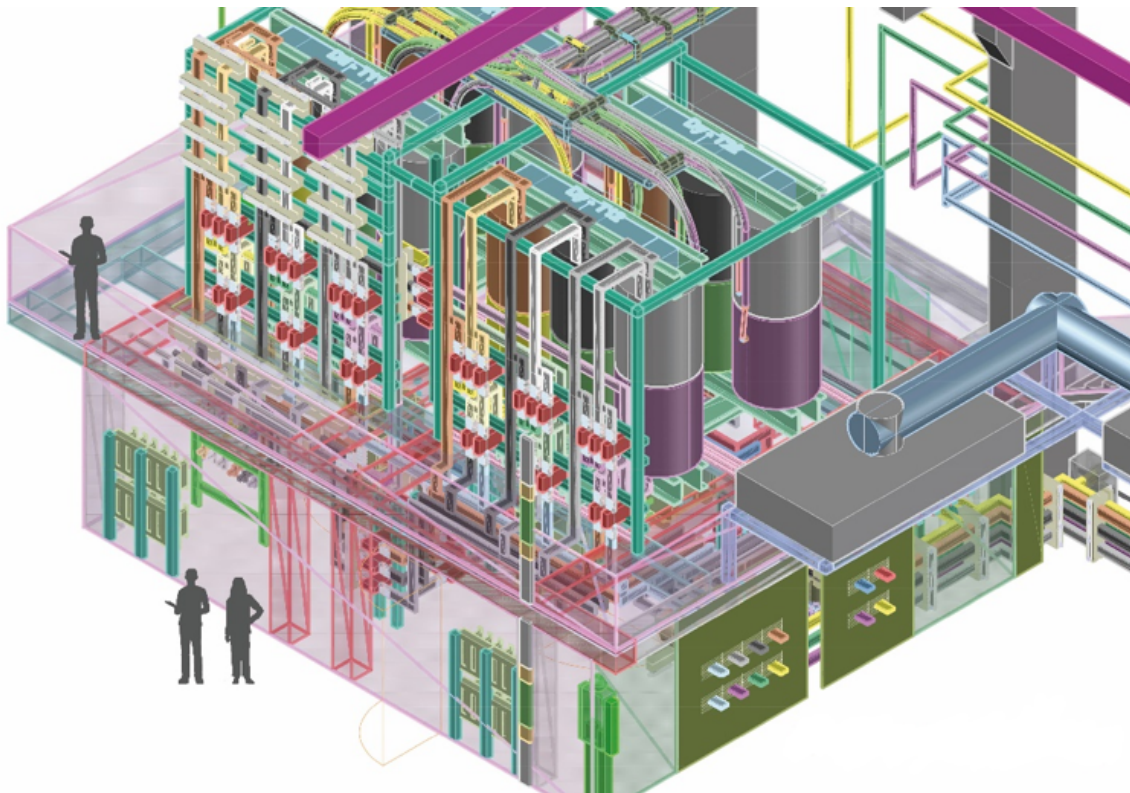


Figure 4: 3-D CAD caption of the MVDC component test infrastructure at AIT.

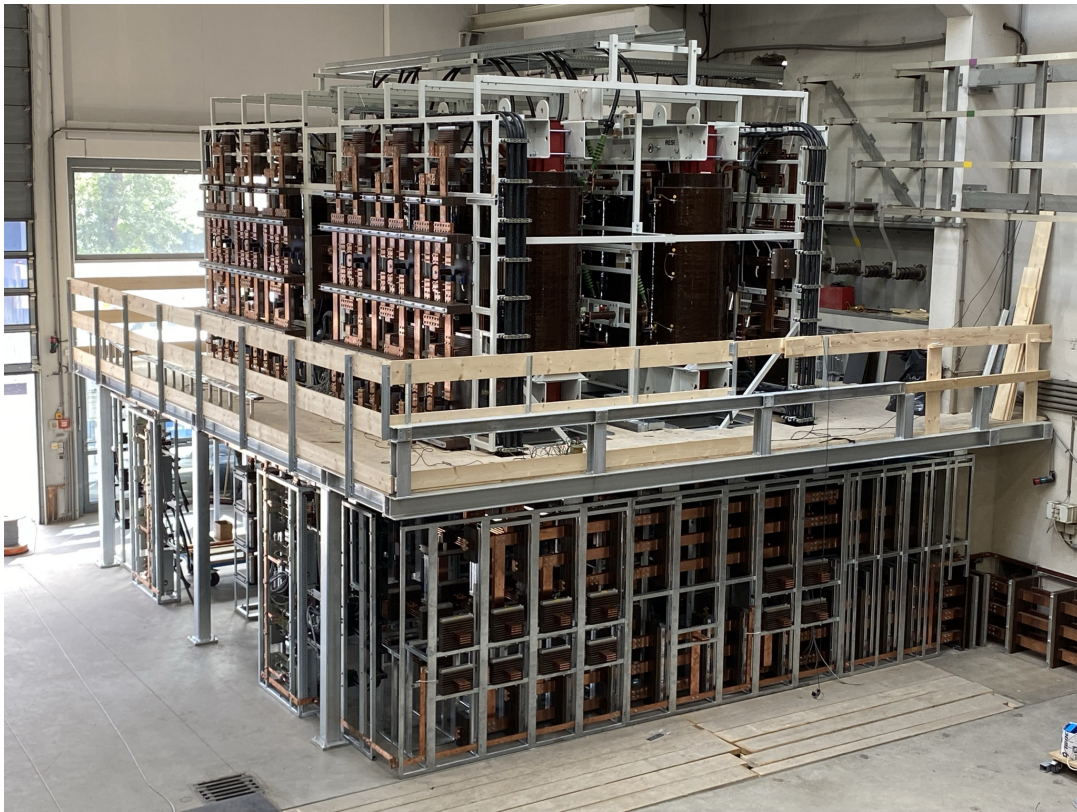


Figure 5: Photographic illustration of the MVDC component test infrastructure at AIT in the building phase showing the high amount of installed copper.



Figure 6: Photographic illustration of the finalised MVDC component test infrastructure at AIT.

2.1.3 Hardware-in-the-Loop (HIL) Laboratory Test at the High-Power Laboratory for Hybrid Grid Components for LV

The AIT SmartEST laboratory is consisting of AC infrastructure with DC sources for tests of grid-connected and offgrid Photovoltaic (PV) inverters. Based on this setup, it is possible to test and validate smart grid components with the state-of-the-art communication interfaces. In addition, prototyping and verification testing of battery and energy storage systems as well as EVSE resulted in an increased demand for testing of DC linked systems and components.

Tests of components may be based on current test procedures since these are already deployed for applications such as PV inverters, battery storage systems or electric vehicle DC charging stations. For each existent DC interface, the Device under Test (DUT) is connected to corresponding power amplifiers and to communication busses in order to test according to predefined test procedures. Depending on the complexity of the testing process, this can also be combined with several iterative parametrisation of respective functions. Within HYPERRIDE these kinds of test procedures will be developed using the AIT SmartEST laboratory which is depicted in Figure 7 and Figure 8.

Subsystem of system tests are based on the simulation of an entire grid section, because it is important to be able to test control algorithm or scaling potential of solutions for smaller networks. Therefore, Power Hardware-in-the-Loop (PHIL), Controller Hardware-in-the-Loop (CHIL), and co-simulation of a real installation with defined interfaces towards larger grids which are simulated in real-time systems enable the assessment of new functions in a potentially unstable environment. To promote these test procedures a LVDC testbed will be conceptualised within the AIT laboratory infrastructure to showcase control and hardware solutions within a safe environment prior to field integration. The general specification in Table 3 is based on the existing SmartEST laboratory installation by AIT.



Figure 7: AIT SmartEST laboratory.

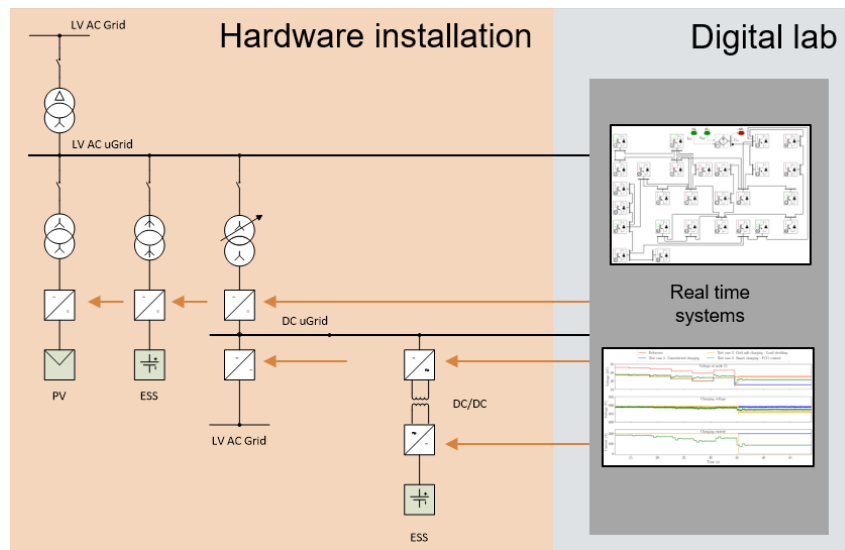


Figure 8: LVDC grid testbed.

Table 3: Functional specification for HIL laboratory test for hybrid grid components (LV).

Function	Description
Grid simulation	3 independent laboratory grids with variable network impedances for up to 1000 kVA, flexible star point configuration and grounding systems
	2 high bandwidth grid simulators: 0 to 480 V 3-ph AC, 800 kVA (AC and DC)
	5 independent dynamic DC array simulators: 1500 V, 1500 A, 960 kVA
	3-phase balanced or unbalanced operation
	Facilities for LVRT and FRT tests
Line impedances	Adjustable set of impedances for meshed, radial or ring network configuration
	Freely adjustable RLC loads up to 1 MW, 1 MVar (capacitive and inductive)
	Individual control of RLC components for performance testing of islanding detection systems
Environmental simulation	Test chamber for performance and accelerated lifetime testing
	Full power operation of equipment under test inside chamber
	Max. size of DUT: 3.60 x 2.60 x 2.80 m (Length x Width x Height)
	Temperature range: -40 degC to +120 degC
	Humidity range: 10% to 98% relative humidity
PHIL simulation	Multicore Opal-RT real-time simulator
	PHIL and CHIL experiments at full power in a closed control loop
DAQ system	Multiple high precision power analyzers with high acquisition rate
	Simultaneous sampling of asynchronous multi-domain data input
General	Indoor and outdoor test areas suitable for ISO containers

2.1.4 HIL Laboratory Test at the Power Electronics (PE) Laboratory for Micro Grid Components

An enhanced laboratory setup consists of two AIT Smart Grid Converter (ASGC) (Active Front End (AFE) mode for AFE1 and AFE2), their respective transformers and one ASGC acting as a load. More detailed information referring to the ASGC operating as AFE is given in the HYPERRIDE Deliverable D3.12, Section 2.

As shown in Figure 9, the two AFEs supply the load on the DC line while the load feeds the power back to the common AC grid. Two defined impedances, Z_1 and Z_2 , are included within the setup to allow for the validation of the implemented droop control. Table 4 provides the values of these impedances.

DC signal measurements are implemented for the AFE1 as well as for the AFE2. However, AC signal measurements are implemented for the AFE2 and the load. All the measurements are filtered through a butterworth filter at a corner frequency of 10 kHz. Figure 10 depicts part of the setup: two ASGCs in a back to back setup, one acting as AFE1, the other as the load.

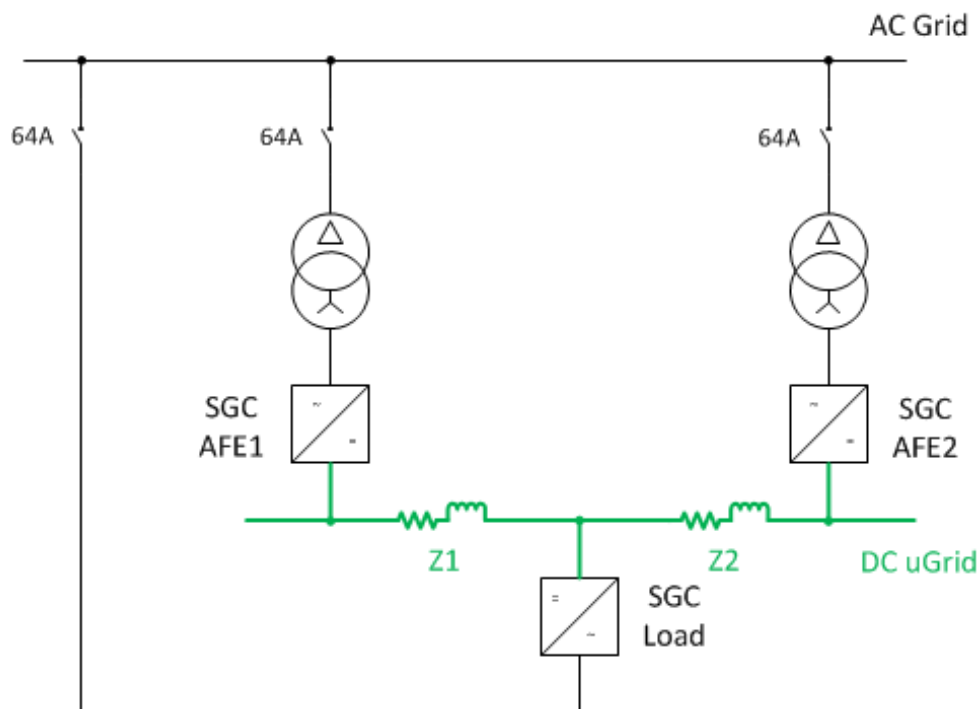


Figure 9: Schematic test setup for active front end validation.

Table 4: Values of the DC line impedances.

Designation	Resistance	Inductance
Z_1	60 m Ω	0.048 mH
Z_2	180 m Ω	1.86 mH



Figure 10: Laboratory setup with two AIT smart grid converters in a back-to-back setup.

Further HIL installations are located in the PE Laboratory involving real-time simulators. The CHIL setup in Figure 11 consists of two Typhoon HIL 602+ emulators connected in parallel and one AIT HIL Controller connected to each Typhoon HIL device. The AIT HIL Controller is developed as a digital twin to ASGC and inside each device is the exact same control board with the same firmware running on it. The controller was also designed to easily interface with the Typhoon HIL emulator. In this setup, the AIT HIL Controller carries out the converter control including the DC droop control while all the other components of the Micro Grid such as electrical grids, transformers, pre-charge circuits, converter power trains are simulated.

The simulation model shown in Figure 12 consists of two ASGCs, AFE1 and AFE2, each connected on the AC side through a transformer to a common AC grid and on the DC side to a shared DC load. Due to a limited number of available processing cores on each Typhoon HIL 602+ device it is not possible to simulate a second ASGC as a DC load. This would require more processing power due to its complexity and a constant current source was used instead.

Between each AFE and the DC load, there is an impedance connected which represents a standard RL section component representing a simplified model of a transmission line with per length resistance, inductance and length parameter. In this model, impedance values measured in the laboratory were used. The SGC component is not part of the standard Typhoon HIL library, but it is a user defined component and represents a model of ASGC's power stage with parameter: nominal power, nominal current and nominal grid voltage. The internal structure of the component consists of a DC bus, a switching bridge, an AC filter, and an AC relay to the grid which are all simulated inside Typhoon HIL emulator. PWM signals and relay control signals on the other hand are not simulated and are coming directly from the controller.

Each Typhoon HIL device has a limited number of processing cores. Therefore, two devices connected in parallel need to be used. AFE1, the connected transformer, the grid simulator, the pre-charge circuit and the DC impedance as well as the DC load are simulated in one Typhoon HIL 602+ device while DC2 and the corresponding transformer are simulated in the other device. Based on this concept, a number of different test cases may be executed with this CHIL setup to investigate system behaviour.

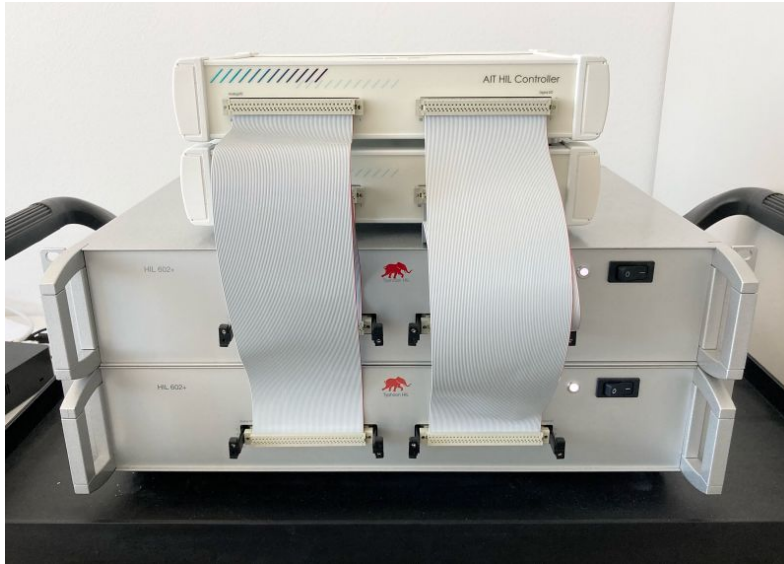


Figure 11: C-HIL setup with two Typhoon HIL 602+ emulators and two AIT HIL controllers.

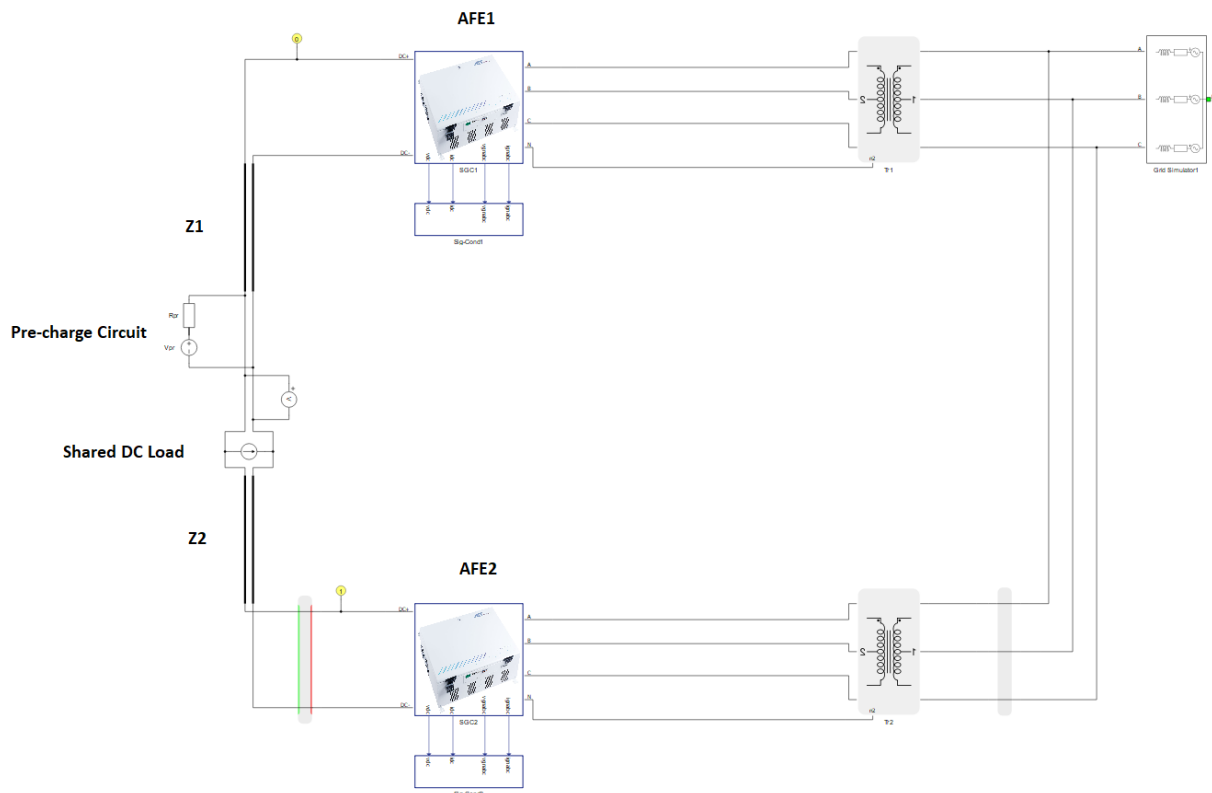


Figure 12: Simulation model for active front end validation

2.2 SCIBREAK

The test circuit used in the SCiBreak laboratory is of a type using a pre-charged capacitor bank. It allows for conducting fault- and load current interruption tests whilst being compact and cost-effective as compared to, for instance, short-circuit current generator.

The schematics of the test setup at SCiBreak's premises is displayed in Figure 13. The capacitor bank, consisting of a number of capacitors $C_1 \dots C_N$, is charged to a predefined voltage level. The stored energy is released into the Test Object (TO) via an inductor L when a making switch $S_1 \dots S_N$ connects the capacitor banks in series with L and TO.

The maximum capacitor voltage is 7 kV and the TIV of the TO is limited by the voltage withstand capability of L to 170 kV. The highest current peak attainable with the test circuit is 19 kA. The maximum energy stored in the circuit is 170 kJ. The component values are summarised in Table 5. The actual test circuit is displayed in Figure 14.

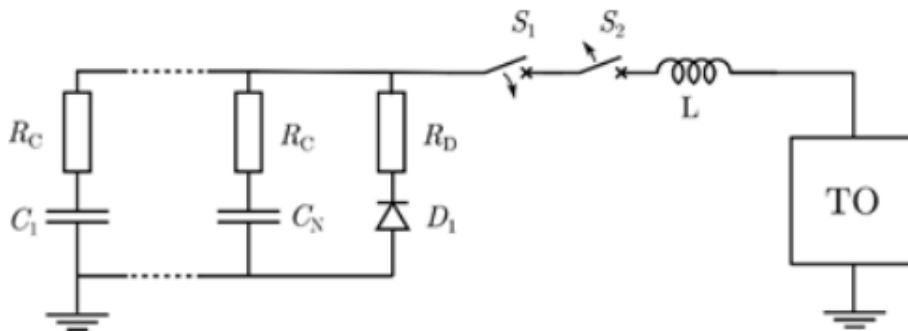


Figure 13: Test circuit connection.

Table 5: Charged capacitor test circuit.

Symbol	Value	Unit	Note
N	10		Number of parallel capacitors
C	690	μF	Unit capacitance
L	800	μH	
R_c	250	$\text{m}\Omega$	
R_d	30	$\text{m}\Omega$	

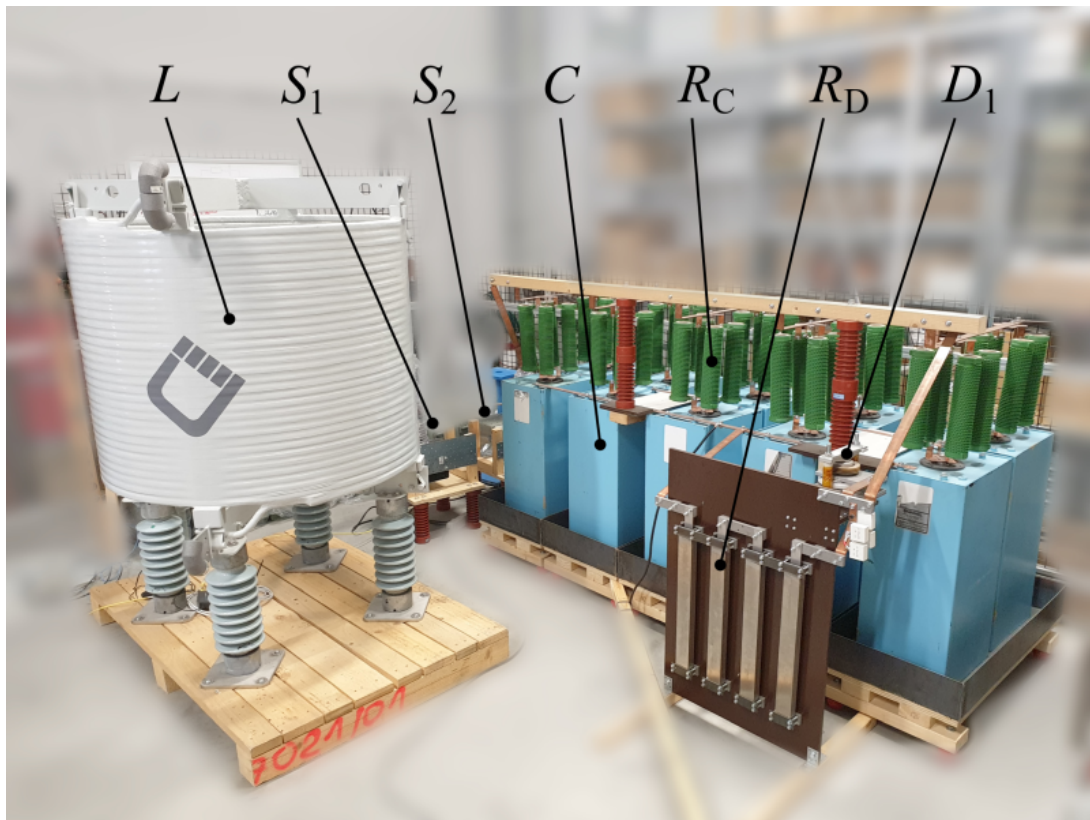


Figure 14: Test circuit.

2.3 EATON

The DC power systems developments in the Eaton European Innovation Center are supported by a dedicated laboratory. The laboratory includes a DC microgrid, with the configuration presented in Figure 15.

The laboratory can be used to test DC microgrid configurations and control algorithms. Controllers can be used to implement centralised (using SG4250 gateway) or decentralised control algorithms (using SMP/4DP gateway). The controller coding can be done in Codesys supported by Eaton controllers, while the control communication is done through Modbus TCP.

The validation of the control algorithms is done by simulation in MATLAB/Simulink and PSCAD for system modelling. A controller hardware-in-the-loop (CHIL) setup can be built to validate the algorithms. The CHIL setup is shown in Figure 16.

Features:

- DER: PV with MPPT 16kW;
- DER: GenSet, Wind (emulated)
- Energy storage: xStorage Home, xStorage Building, 20-40kWh.
- Bidirectional Active Front End 37kW.
- Bidirectional EV charger.
- EEIC building control integration;
- DC bus +700V, (+/-350V, +/-700V);

2023

- Bidirectional EV charger.
- EEIC building control for benefit assessment.

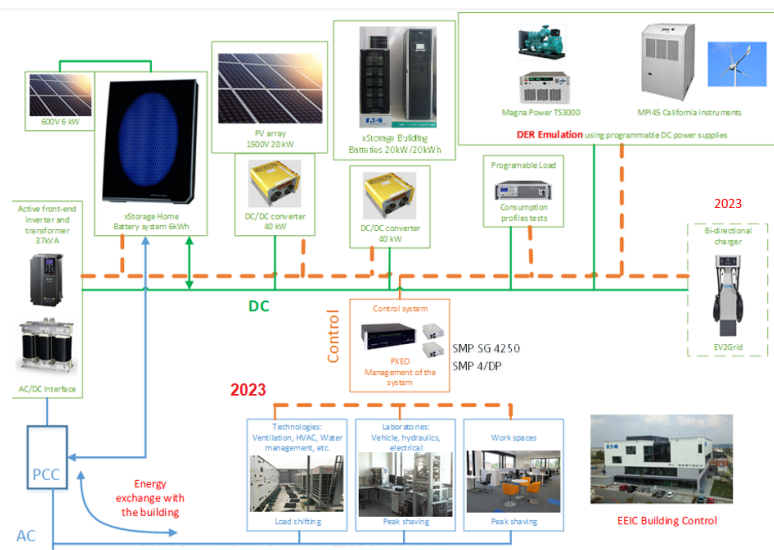


Figure 15: Eaton DC power systems laboratory.

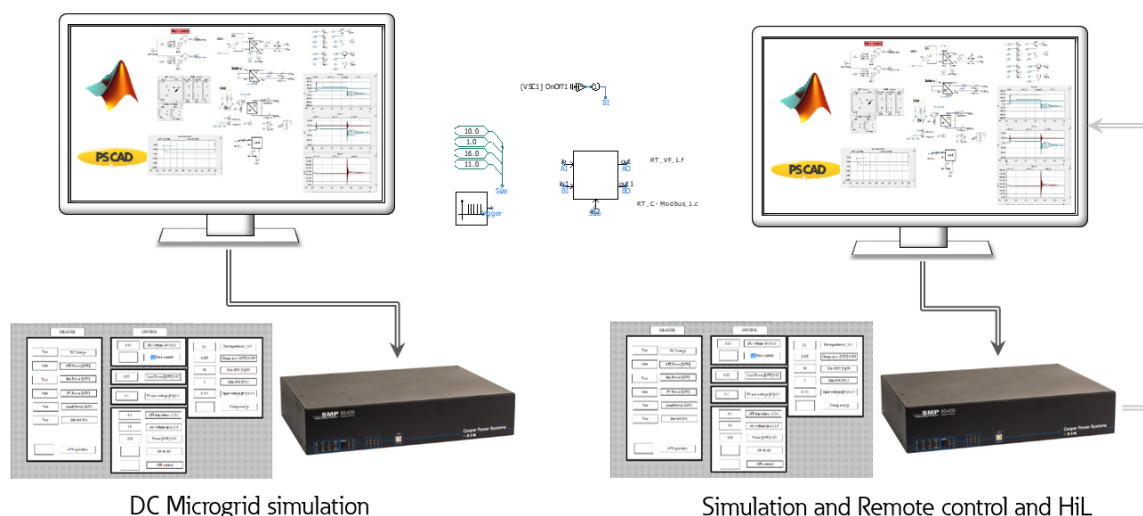


Figure 16: Controller Hardware-in-the-Loop (CHIL) setup.

For the development of the 14 kV MVDC hybrid circuit breaker, a Thomson Coil Actuator (TCA) was designed and a prototype was built. The functional testing of the TCA was performed with a custom made circuit, as in the LTSpice schematic shown in Figure 17. The circuit is used to charge the capacitor to 800 V, which is then discharged through the TCA opening coil. During this test, a current pulse of 10 kA peak and 0.7 ms duration is generated, for a fast actuation (9 mm contact displacement, in 2 ms). The actual testing setup and the functional PCBs are shown in Figure 18.

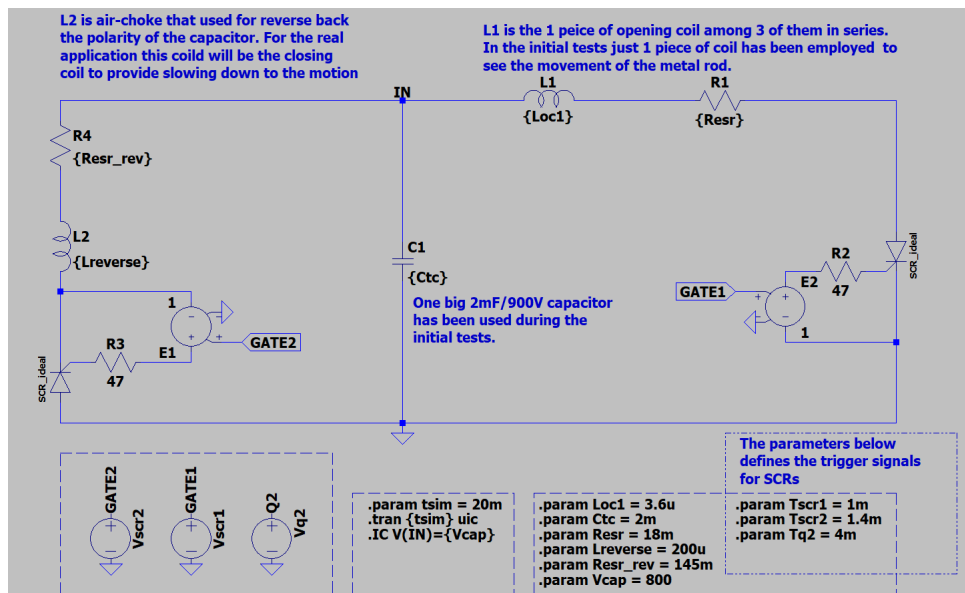


Figure 17: LTSpice schematics of the circuit used for TCA opening tests.

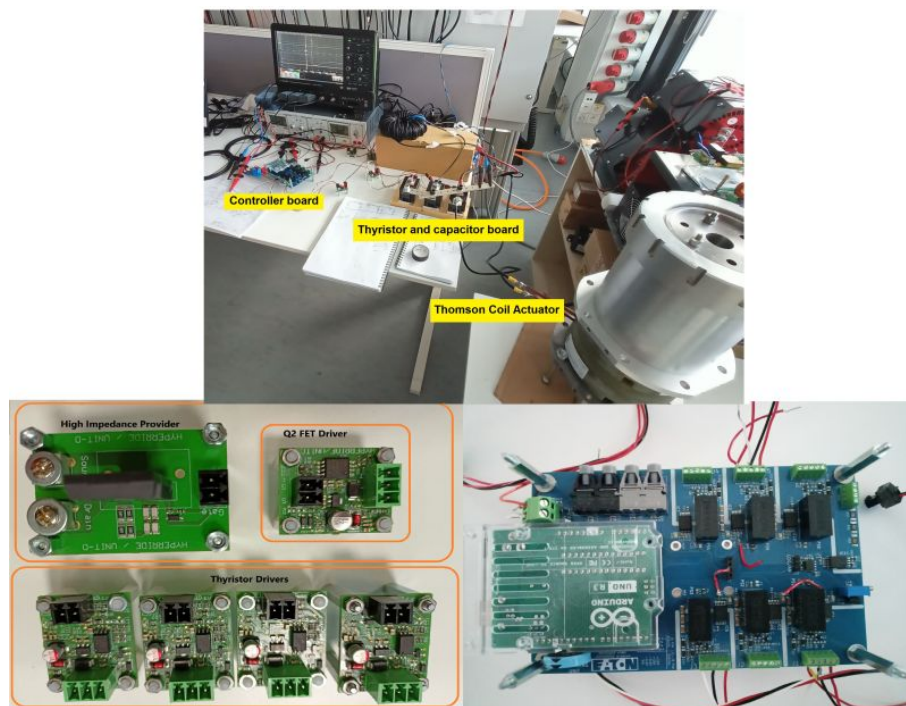


Figure 18: Testing setup for functional verification of the TCA prototype.

2.4 RWTH Aachen

At RWTH Aachen University, a hybrid MV/LV AC/DC microgrid is developed for the HYPER-RIDE project. Figure 19 depicts a scheme of the infrastructure. The grid consists of different MV and LV converters that were bought from various manufacturers and are partly self-built. The microgrid also includes the ± 2.5 kV FEN research grid. The flexible grid set-up allows to test converter control and protection concepts. To enable the global control of the microgrid, a Supervisory Control and Data Acquisition (SCADA) system was developed and the control structure of each converter was extended to a unified set of functionalities, in order to achieve interoperability. Commissioning the microgrid consisted of different tasks:

- MV AFE and the 3-phase Dual Active Bridge (DAB) (Insulated Gate Bipolar Transistor (IGBT) DAB3).
- Single-phase MV-LV DAB (DAB1).
- Modular three-phase DAB (Modular DAB3).
- LV AFEs (LV AC AFE).

During the commissioning process of the converters, first the connection of the converter control to the SCADA system was tested. After verifying the the operation of the communication structure, the control functionalities of each converter were tested, as shown in Figure 20.

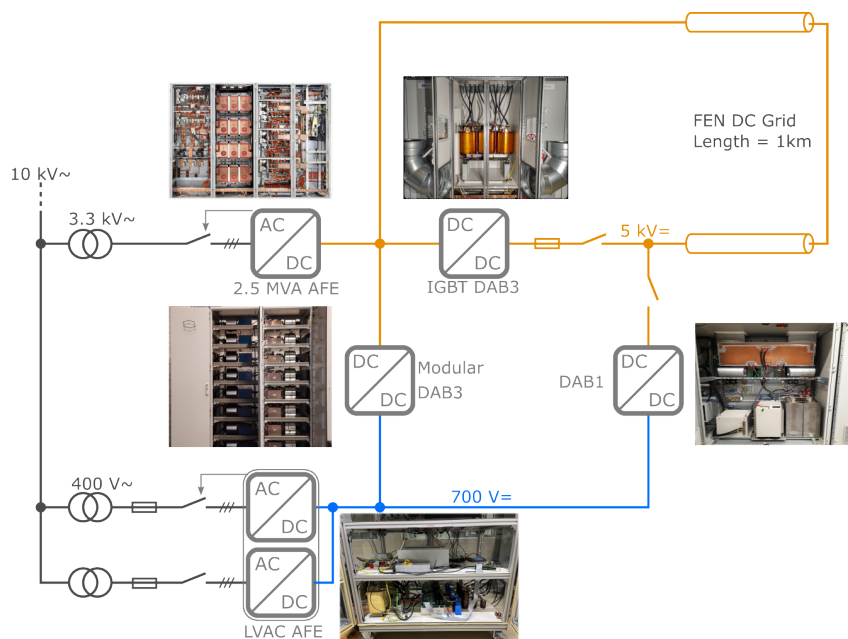


Figure 19: Overview of the hybrid MV/LV AC/DC microgrid.

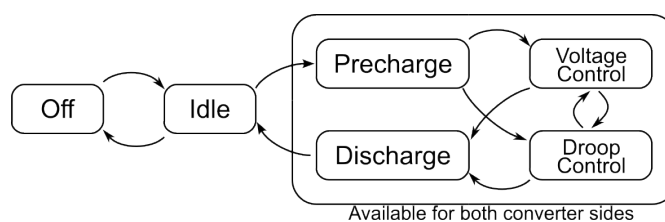


Figure 20: Overview of the different control functionalities of the converters.

2.5 EPFL

At EPFL, an LV AC/DC microgrid is developed for the HYPERRIDE project. In Figure 21, a scheme of the infrastructure is sketched. Figure 22 shows equipment for converter commissioning and Figure 23 depict the converters to be commissioned. The AC microgrid, already in service for more than 10 years, is connected to 4 newly serviced DC lines using 45 kW-rated active front end (AFE) converters. The interconnection of those DC lines is done using different DC/DC converters, with different topologies (Dual Active Bridge (DAB) or LLC converters). At each DC line, different DC loads and sources can be connected, such as 15 kW PV emulators.

Commissioning the DC grid consisted in different sub-commissioning tasks:

- Commissioning of the AFEs.
- Commissioning of the DC Transformer (DC/DC converter based on LLC topology).
- Commissioning of the PV emulator.

The Power Electronics Laboratory (PEL) is in charge of the commissioning of the DC part of the grid and has different equipment to allow full commissioning of the converters. Below are a few pictures of the available equipment:

- Regatron TC.ACS : 200 kW grid emulator, AC and DC bidirectional power source.
- Chroma: small AC power supply (small power ratings).
- Power supply high current, low voltage (Sorensen 125 A, 10 V).
- AC load: 25 kW.
- Delta power supply.

AFE commissioning:

- Sensor calibration: current sensing procedure. The Delta power supply supplies the DC link of the AFE to energise the controller (controller supply comes from the DC-link voltage) and the Sorensen power supply, in current mode, is connected to the DC-link negative point and to one of the inverter's leg. The leg is short-circuited by a 0 duty cycle reference provided by the controller.
- Test of the current control loop: Regatron AC grid emulator connected to the AC terminals of the rectifier, AC load is connected to the inverter AC terminals.
- Test of the DC current control loop: no power: Regatron AC grid emulator connected to the inverter AC terminals and to the rectifier AC terminals (for initial DC-link charging). Test can be performed with maximum reactive power point (almost 45 kVA).
- Test of the DC current control loop with power: power circulation test with 2 AFEs, 1 DCT.

DCT commissioning, two configurations are possible:

- Power circulation test 1: 1 DCT, 1 current source (low voltage, high current), 1 DC power supply (low power, unidirectional).
- Power circulation test 2: 1 DCT, 2 DC power supplies (high powers, bidirectional).

With those two configurations, the commissioning of all the functionalities of the DCT is possible: power reversal, soft-start, current limiting function. PV emulator commissioning: the procedure is very similar to the AFE commissioning procedure.

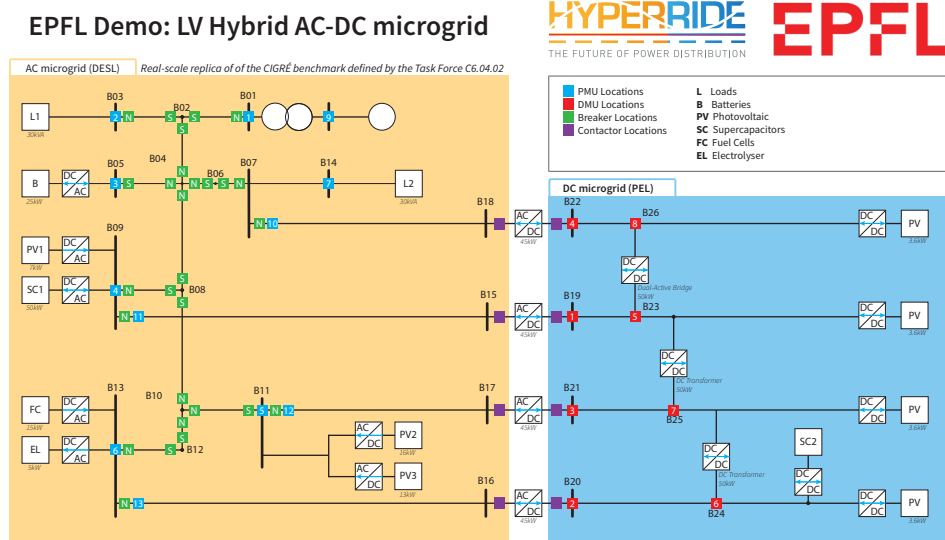


Figure 21: Scheme of EPFL demonstration site.



Figure 22: Equipment for converter commissioning.

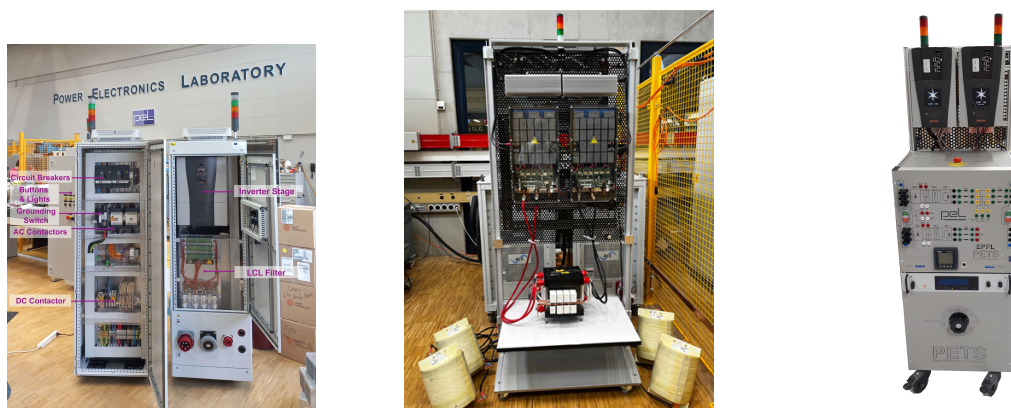


Figure 23: Converters to be commissioned.

2.6 ZELISKO

This chapter presents a detailed description of the available test methods at Zelisko, which are subsequently used for current and voltage sensing. Regarding the current sensor, a distinction has to be made between the actual sensor and the signal conditioning board. The following DC power supplies are used for test setups for the signal processing board: TDK Lambda (150 V, 5 A), Sorensen XPD series (33 V, 16 A), GW Instek PSU 6-200 (200 A, 6 V).

To ensure that current and voltage sensors are free of partial discharge, Zelisko uses the measurement setup shown in Figure 24 with maximum voltage and power ratings of the PD-measurement setup given by 200 kVac, 20 kVA, respectively. In Figure 25, the general structure of the measuring bridge used for precise AC current measurement is shown. The measurement range of the current transformer can be switched in steps what results in an adjustable current range of 5 A to 5 kA on the primary side and 1 A to 5 A on the secondary side, respectively.

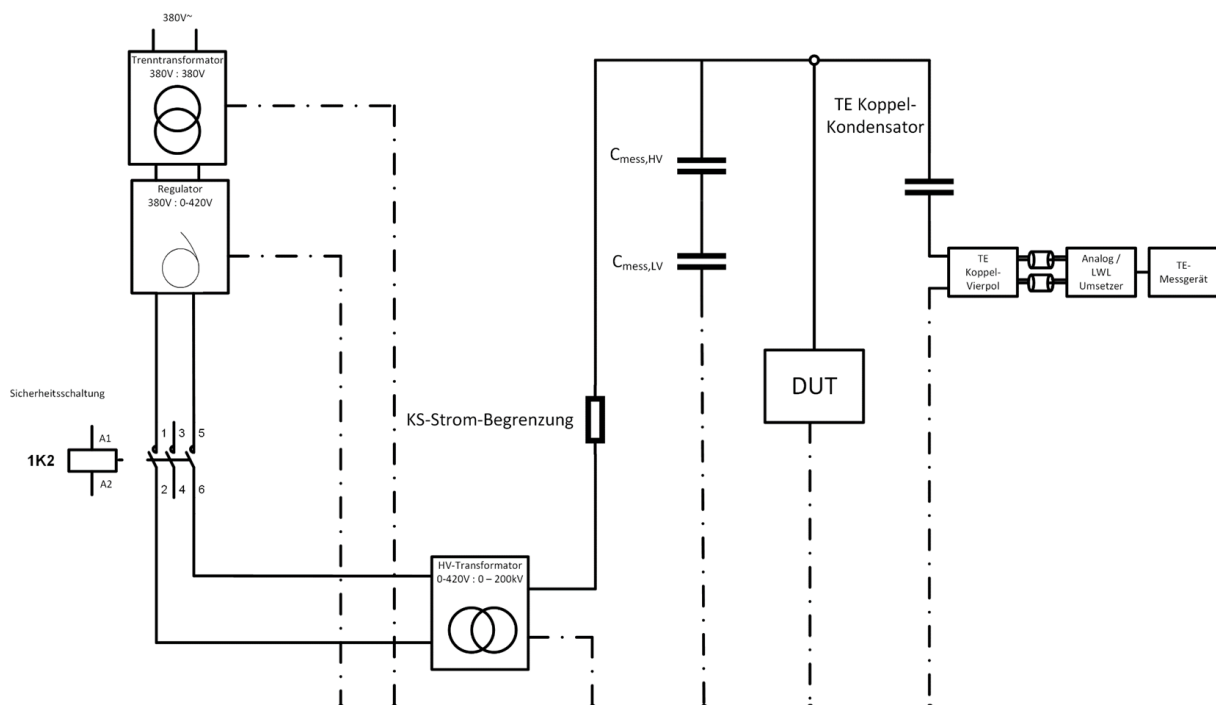


Figure 24: PD-measurement setup.

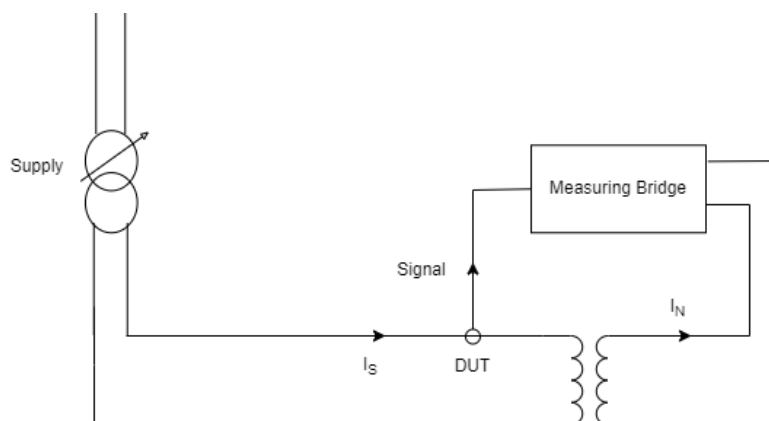


Figure 25: Current measuring bridge.

For the temperature compensation measurements a environmental test chamber (company: CTS) with a temperature range of $-70\text{ }^{\circ}\text{C}$ and $+180\text{ }^{\circ}\text{C}$ has been used. Figure 26 (left) presents a photographic illustration of the experimental setup which uses the environmental test chamber, the PSU 6-200 for the primary current generation, and the Keithley 2000 for the output voltage measurement. In this setup, the sensor has been tested for a temperature range between $-25\text{ }^{\circ}\text{C}$ and $+55\text{ }^{\circ}\text{C}$. In Figure 26 (right), a photographic illustration of the setup in the environmental test chamber is depicted.



Figure 26: Temperature compensation setup (left); Hall sensor in the environmental test chamber (right).

Figure 27 shows a schematic for an experimental setup to determine the offset in dependence of the mechanical force (Holzbauer, 2023). The Hall offset is influenced by external magnetic fields, temperature as well as mechanical force which also applies during the epoxy casting. The load cell was mechanically fixed in the spindle. The shaded rectangles define wooden blocks that were positioned around the Hall element.

The wooden blocks were used for various reasons. On the one hand, the Hall plate and placeholder are positioned in the air gap of the core. The mechanical forces generated during the curing of the epoxy resin would thus primarily affect the iron core and not the Hall element directly. Therefore, the wooden blocks represent the iron core surrounding the Hall element. Furthermore, without the wooden blocks, the Hall sensor would be destroyed within a very short time or the individual Hall element contacts, which are necessary both for the supply and for the output signal, would break. The black rectangle between the wooden blocks thus defines the Hall element. In total, two different supply voltages are needed, one for the Hall element and one for the load cell. The measurement outputs of the load cell and the Hall sensor are then connected to the data logger. By rotating the spindle, the device together with the load cell then moves in the direction of the Hall element. The force was applied centred on the wood block, which should not result in any displacement of the wood block. To avoid possible displacement due to a non optimally aligned load cell, wooden plates of approximately the same thickness as the placeholder of the Hall element were attached to the edge between the wooden blocks.

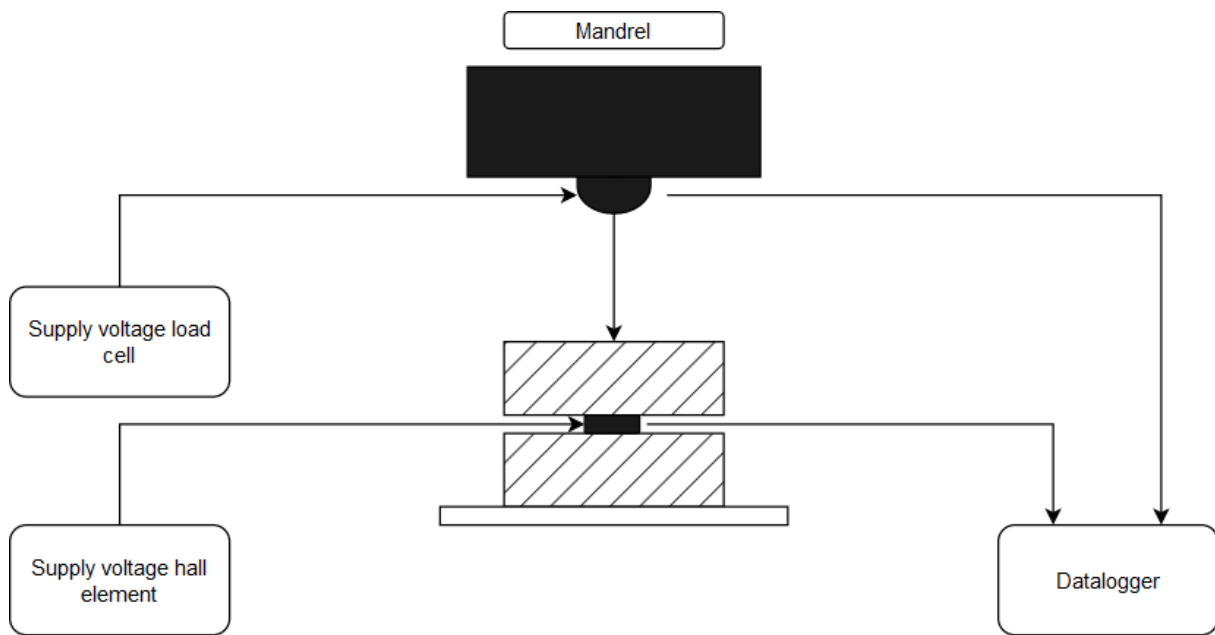


Figure 27: Schematic of the experimental setup for mechanical force measurements.

The DC accuracy measurement setup is illustrated in Figure 28. The first power supply unit is the DC power supply, which provides a maximum output current of 200 A. The connection between the power supply unit and the prototype is made via copper rails. The second power supply in the schematic design denotes the different power supplies, which are used to provide the positive as well as the negative supply voltage for the transistors and the operational amplifier. The four outputs for the Hall element integrated in the prototype are connected to an interface PCB board, the so-called "Perfboard" (see Figure 28). Furthermore the two winding ends are connected to the board. The first winding connection supplies the compensation current amplified by the Perfboard to the prototype. The second winding terminal is connected in series with the shunt resistor placed on the board. The voltage across the shunt resistor is then measured using the Keithley 2000 multimeter.

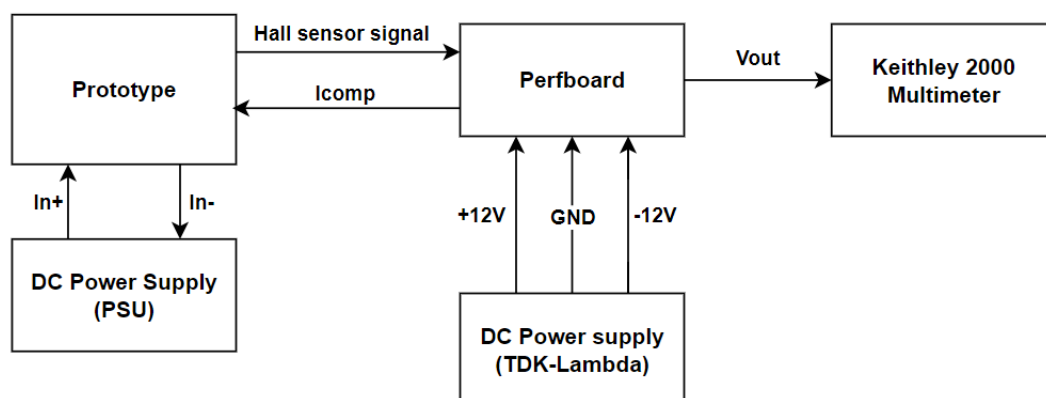


Figure 28: DC accuracy measurement setup.

2.7 EMOT

EMOTION is a charging station manufacturer, charging point operator, electric mobility service provider and it is the responsible partner for developing DC/DC FAST charging station to be deployed in Terni pilot site. For this purpose, Zekalabs RedPrime DC/DC Converter 40 kW depicted in Figure 29 and given specifications in Table 6 has been selected and tested in EMOT lab environment; Zekalabs RedPrime DC/DC Converter 40 kW satisfies Terni pilot DC grid voltage requirements and it enables bidirectional power flows for vehicle to grid functionality.

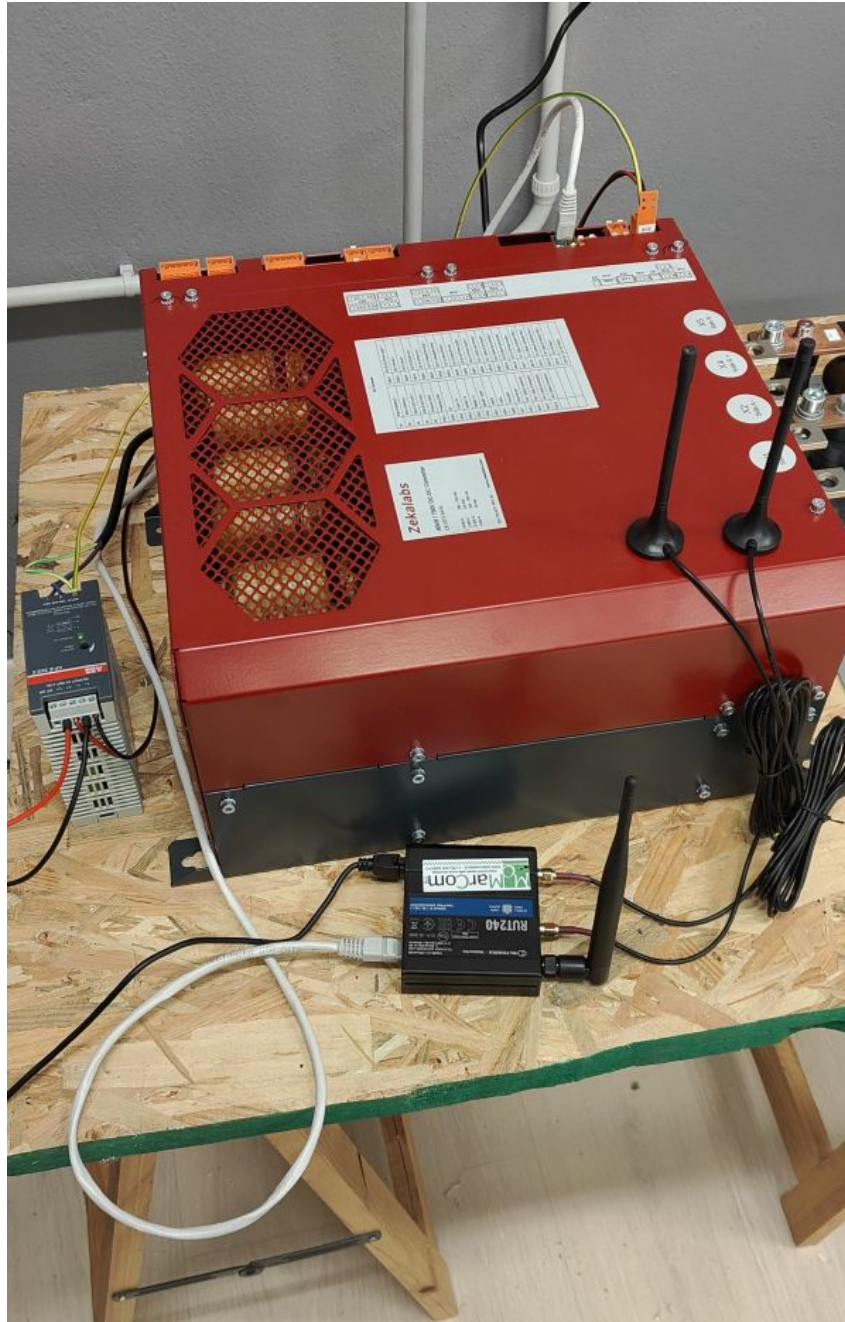
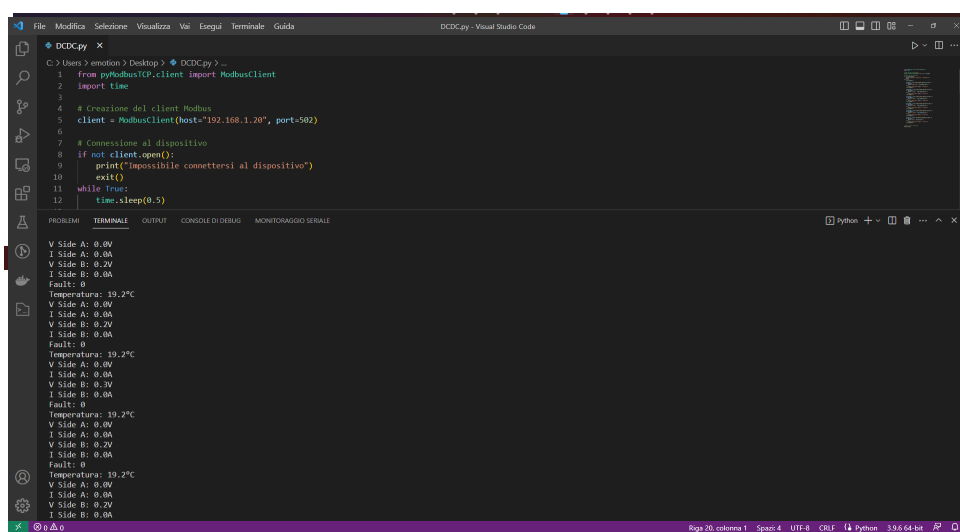


Figure 29: Zekalabs RedPrime DC/DC converter 40 kW, 750 V lab testing.

Converter high-voltage side has been set to 700 Vdc for the connection with Terni DC grid meanwhile low-voltage side has been set to 400 Vdc for electric vehicle charging/discharging. Zekalabs LB-1111-01 contactors block has been selected as contactor solution; it consists of a precharge resistor shown in Figure 30, precharge contactor and a main contactor plus convenient terminals for wiring with the converter (see Figure 31, Table 7).

Table 6: Technical specifications of the Zekalabs RedPrime DC/DC converter.

Characteristics	Value
Nominal Power	40 kW
Min Side A (low-voltage side) voltage	10 Vdc
Max Side A (low-voltage side) voltage	700 Vdc
Max Side A (low-voltage side) current	120 Adc
Min Side B (high-voltage side) voltage	Low voltage Side A + 50 Vdc
Max Side B (high-voltage side) voltage	750 Vdc
Max Side B (high-voltage side) current	60 Adc
Efficiency	> 98% (load power > 20%)
Energy transfer direction	Bidirectional - buck and boost
Switching Frequency	18 kHz
Side B (high-voltage side) capacitance	240 μ F / 700 V
Cooling	Forced air - internal fans
Cooling air flowrate	150 l/min or 9 m ³ /h
Power supply voltage	24 Vdc \pm 10%
Power supply current with fans on	< 2 A
Power supply current with fans off	< 1 A
Degree of protection	IP22
Mechanical dimensions (W x L x H)	350 x 400 x 186 mm
Weight	28.5 kg
Operating temperature	-20 °C to 50 °C (derating over 50 °C)
Humidity	96 %, not condensing
Enclosure	Zn plated steel sheet, powder painted Aluminum



```

1 from pyModbusTCP.client import ModbusClient
2 import time
3
4 # Creazione del client Modbus
5 client = ModbusClient(host="192.168.1.20", port=502)
6
7 # Connessione al dispositivo
8 if not client.open():
9     print("Impossibile connettersi al dispositivo")
10    exit()
11 while True:
12    time.sleep(0.5)
  
```

```

PROBLEMI TERMINALE OUTPUT CONSOLE DI DEBUG MONITORAGGIO SERIALE
V Side A: 0.0V
I Side A: 0.0A
V Side B: 0.2V
I Side B: 0.0A
Fault: 0
Temperatura: 19.2°C
V Side A: 0.0V
I Side A: 0.0A
V Side B: 0.2V
I Side B: 0.0A
Fault: 0
Temperatura: 19.2°C
V Side A: 0.0V
I Side A: 0.0A
V Side B: 0.2V
I Side B: 0.0A
Fault: 0
Temperatura: 19.2°C
V Side A: 0.0V
I Side A: 0.0A
V Side B: 0.2V
I Side B: 0.0A
Fault: 0
Temperatura: 19.2°C
  
```

Figure 30: DC/DC converter registers reading.

Modbus TCP communication over Ethernet interface has been adopted for the converter control. As shown in Figure 32, Figure 33 and Table 8, SETEC POWER AC/DC converter model SDC450 has been selected for DC/DC converter lab testing.

Table 7: Technical specifications of the Zekalabs LB-1111-01 contactors block.

Characteristics	Value
Power supply voltage	24 Vdc \pm 10%
Length	330 mm
Width	253 mm
Height	88.5 mm
Weight	4.0 kg
Degree of protection	IP20
Operating temperature	-20 °C to 50 °C (derating over 50 °C)
Humidity	96 %, not condensing
Enclosure	Zn plated steel sheet

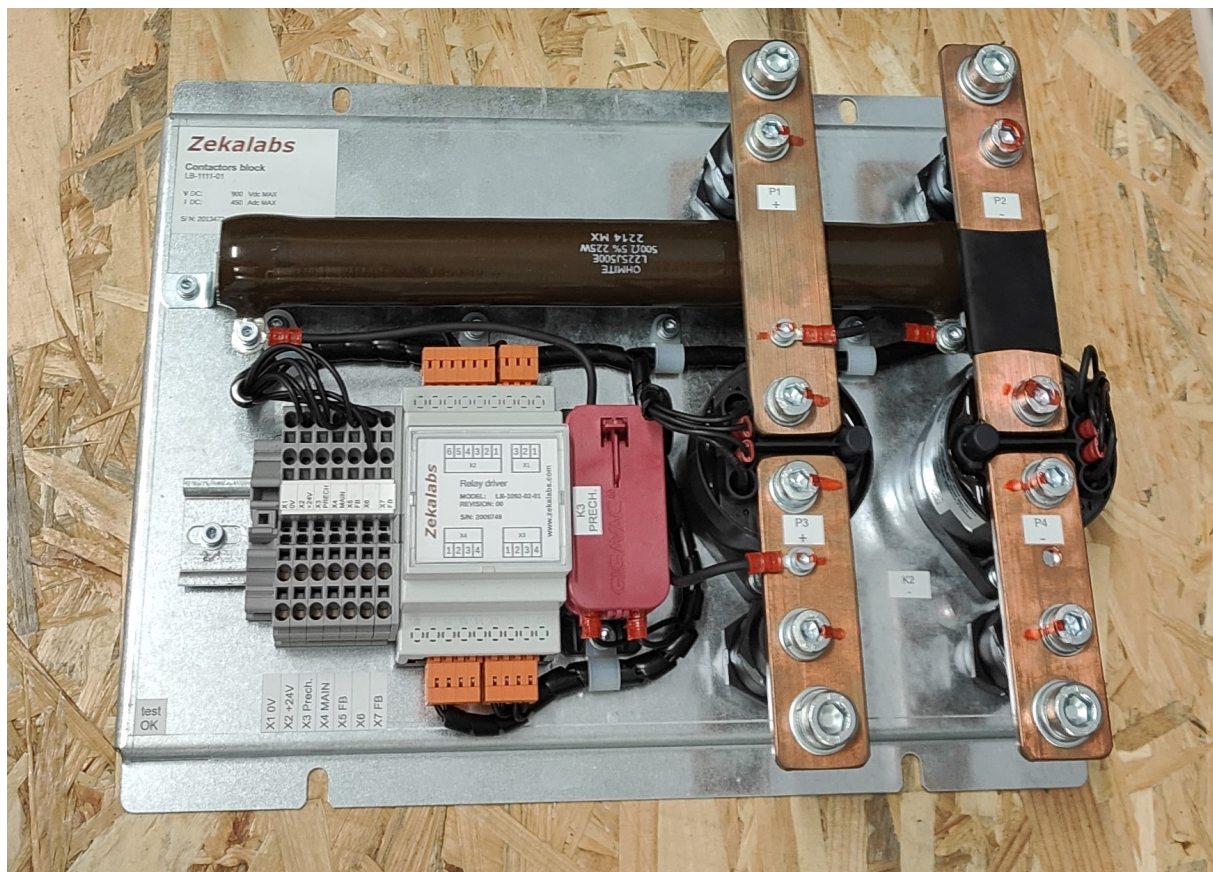


Figure 31: DC/DC converter contactors block.

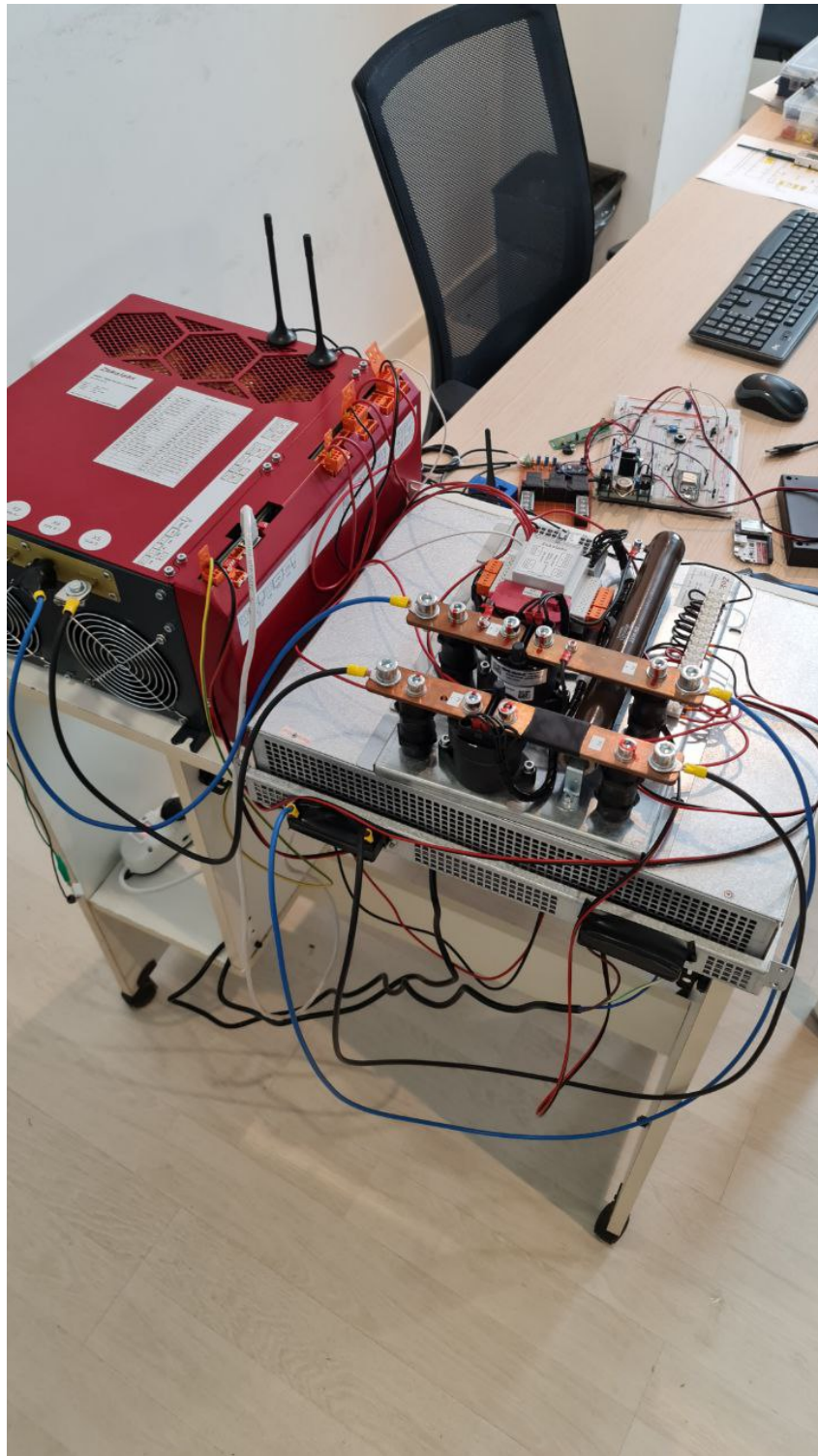


Figure 32: DC/DC converter connected to contactors block and AC/DC converter for lab testing.

Table 8: Technical specifications of the SETEC POWER SDC450 AC/DC converter.

Characteristics	Value
Input Voltage	305-520 Vac
Frequency	40-65 Hz
Output Voltage	100-450 Vdc
Max Output Current	23 A
Rated Output Power	10 kW
Regulation Accuracy	$<\pm 0.5\%$
Precision of Steady Current	$<\pm 1\%$
Ripple Factor	$<\pm 0.5\%$
Efficiency	$>95\%$ (Load: 50 - 100%)
Power Factor	>0.99
Unequal Current Ratio	$<\pm 5\%$
Dielectric Strenght	IVP input&output, input&chassis 2000 Vac, 1 min, No breakdown, no flashover; IVS input,output &chassis 1000 Vac, 1 min, No breakdown, no flashover
Insulation Resistance	1000 Vdc, $>10\text{ M}\Omega$
Degree of protection	IP21
Size (mm)	374 (D) x 482 (W) x 88 (H)
Weight	13 kg
Communication Port	RS485/CAN
Operating temperature	$-25\text{ }^{\circ}\text{C}$ to $65\text{ }^{\circ}\text{C}$
Storage temperature	$-40\text{ }^{\circ}\text{C}$ to $70\text{ }^{\circ}\text{C}$
Humidity	Working $<90\%$, Storage $<95\%$



Figure 33: AC/DC converter for lab testing.

A cabinet 60x60x170 cm (LxWxH) with IP54 protection degree will be used to host DC/DC FAST charging station equipment shown in Figure 34.



Figure 34: DC/DC charging station cabinet.

Internet connection will be granted by a Teltonika router and a Raspberry Pi 3 will be used to run EMOT management system. Finally, five fans with 120 mm diameter will be used for cabinet cooling depicted in Figure 35.

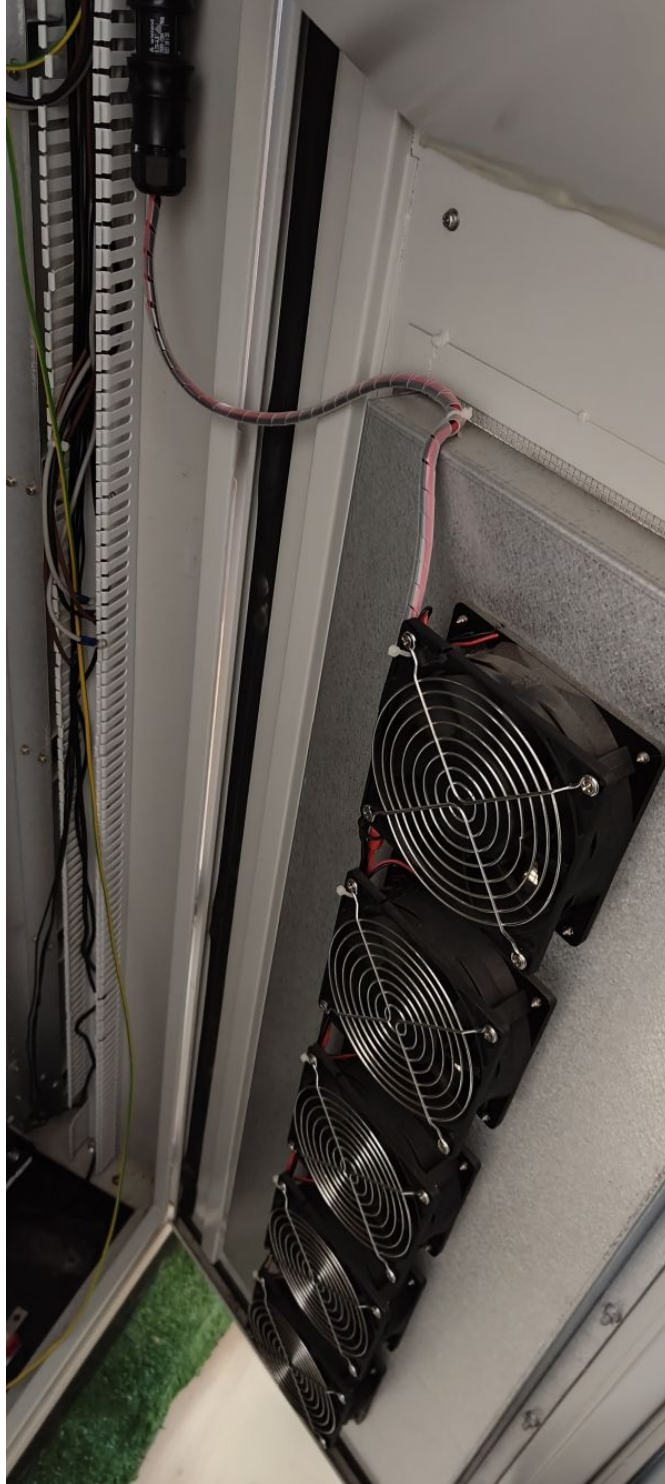


Figure 35: DC/DC charging station cabinet forced air ventilation.

Furthermore, an electrical vehicle interface (EVI) has been installed to enable EV charging; EVI is a dual standard supply equipment communication controller (SECC) with required signals for CCS2/Combo (DIN SPEC70121, ISO15118-2, ISO15118-20) and CHAdeMO communications. In particular, Watt and Well SECC has been selected; it is compliant with IEC 61851-23 and IEC 61851-1 requirements subsets for SECC, as well as it manages V2G charging modes CHAdeMO BPT and CCS V2G (via ISO15118-20).

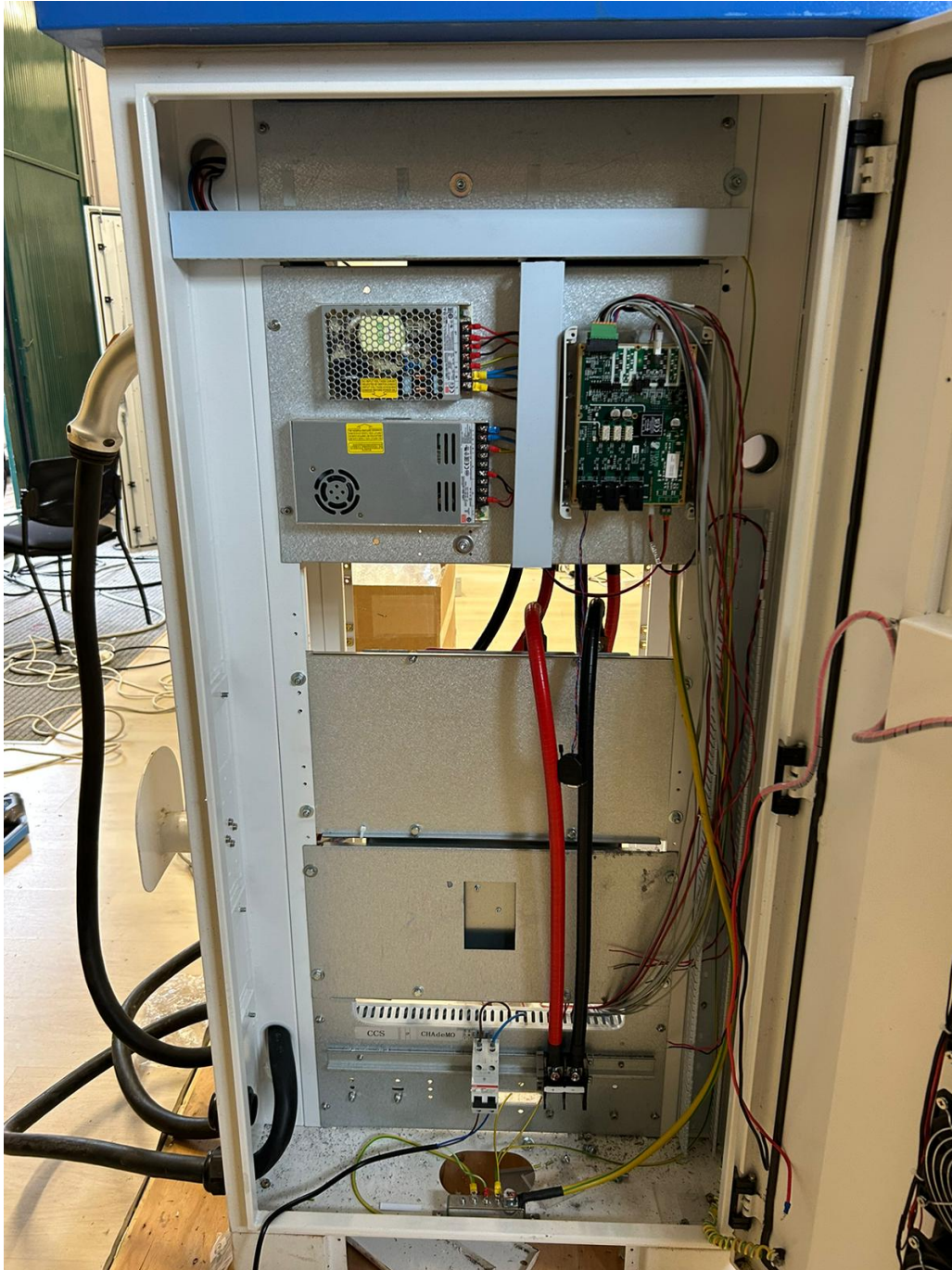


Figure 36: DC/DC charging station EVI.

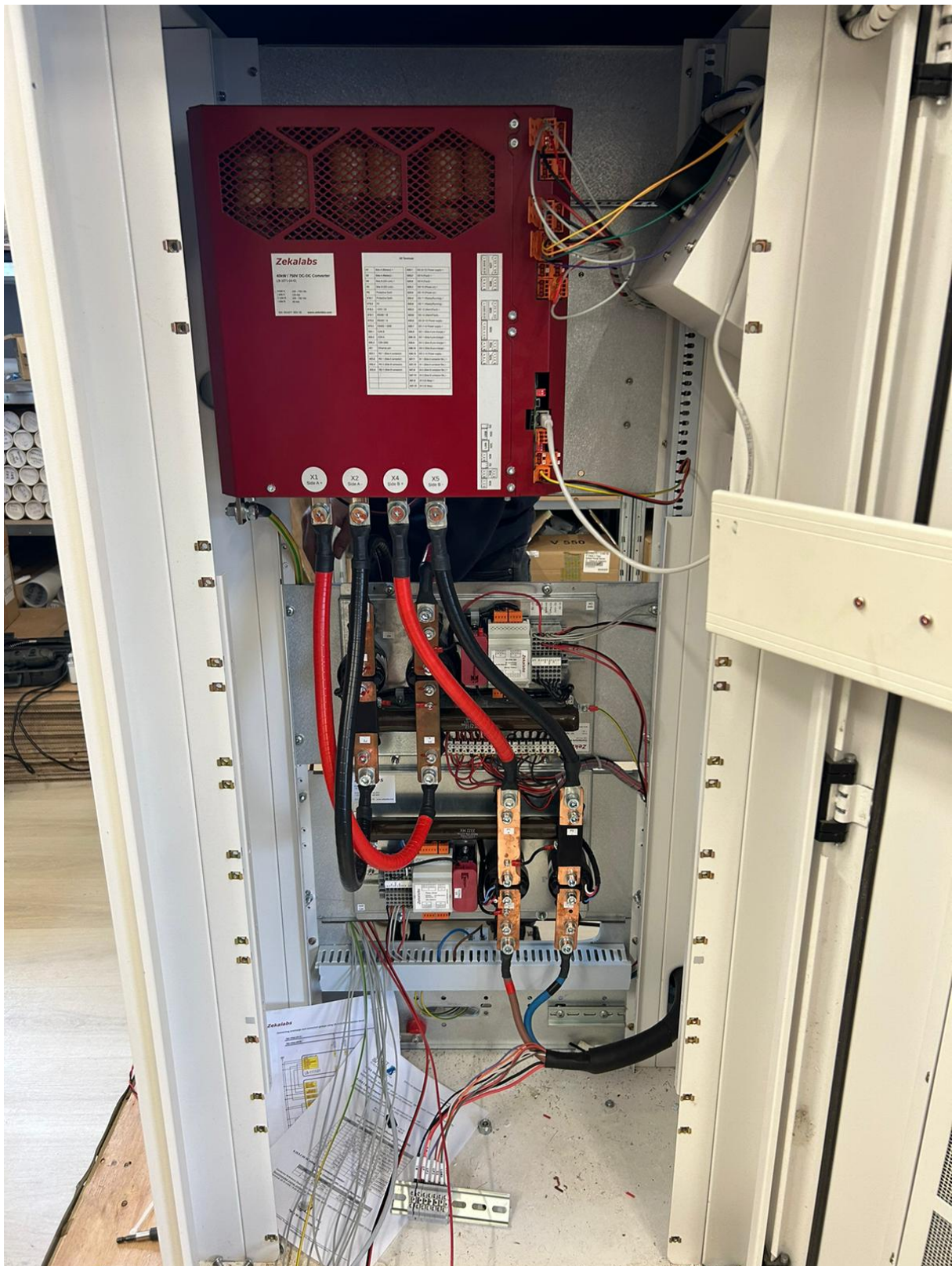


Figure 37: DC/DC charging station converter installed in the cabinet.

2.8 ASM Terni

The Italian pilot develops a hybrid AC/DC distribution grid that combines the needs of users with those of the Distribution System Operator to limit congestion at grid nodes and promote local self-produced energy consumption. The use of converters, protections, measuring devices and control systems, some of which are supplied by the project partners, is based on the reliability and multi-operability requirements of all the systems involved. The aim of the pilot is to build a test bed to validate technologies that can be used in AC/DC hybrid grid applications.

Physically, the Italian pilot consists of a 700 Vdc section inserted into a portion of the existing LV distribution grid in the city of Terni. Electric diagram, PV plant, active front end converters, storage and PV supplies, second life cycle batteries, and DC grid control are shown in Figure 38 - Figure 42, respectively. The DC busbar is fed through two AC/DC converters, each connected to a different Secondary Substation: SCOV and ASM. The following units are connected to the DC busbar: electric vehicle charging station, PV system, storage systems, critical loads.

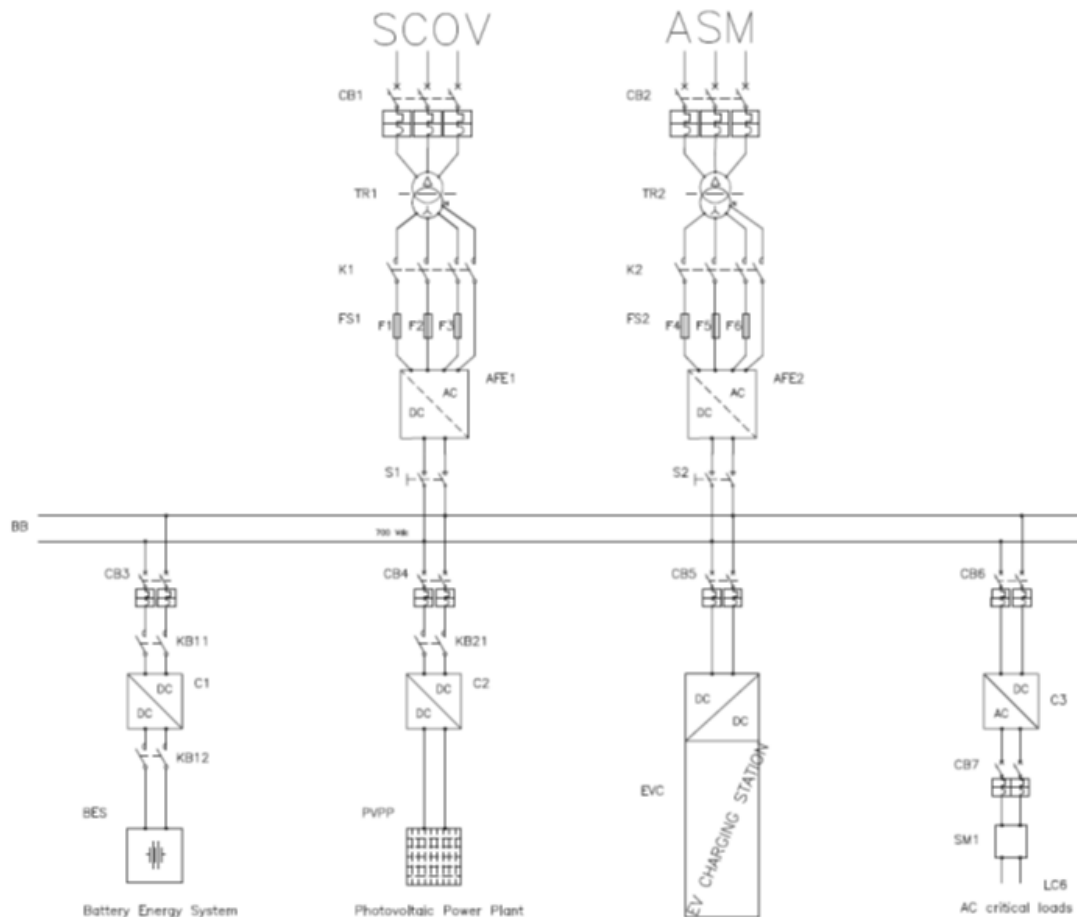


Figure 38: Italian pilot - electric diagram.

A new PV power plant was installed in the pilot site to supply green power to the DC busbars. The PV system consists of 2 strings in parallel, each composed of 18 panels in series. Each panel, at maximum power, i.e., at the highest level of solar irradiation, delivers a voltage of 34.3 V. At open circuit, i.e., when the panel terminals are not connected to a load, the voltage is 41.2 V. Consequently, the voltage delivered to the DC/DC converter is: $18 \times 34.3 = 617.4$ V. The total peak power output of the PV system with the two strings in parallel is 12 kW. The

fluctuating DC voltage of the PV panels is regulated to 700 Vdc by a DC/DC converter. The main DC busbars are supplied by two Active Front End Converters manufactured by AIT. Each converter can supply a maximum power of 35 kW. Therefore, the system receives 70 kW as total power from the AC grid from two Secondary Substations (ASM and SCOV).



Figure 39: Italian pilot - photovoltaic power plant.



Figure 40: Italian pilot - active front end converters.

The main power supply system is completed by the storage and photovoltaic converters mounted next to each other in the same switchboard.



Figure 41: Italian pilot - storage and photovoltaic DC power supply.

The storage system is provided by EATON and is based on the use of second-life batteries from the electric vehicle industry.



Figure 42: Italian pilot - second life cycle batteries.

A Synchronised Measurement Unit (SMU) made by RWTH is integrated in the Italian pilot site. The SMU is a DC measurement device with a dedicated data acquisition unit to collect data on up to eight channels. Each SMU summarises information and provides experimental data.

A local control manages the DC functional units of the demo site to optimise the power flow and maximise the local consumption of the energy produced by the photovoltaic system. The control system developed by EATON also assesses the state of charge of the batteries and any electric vehicle charging needs.

The electric vehicle charging station is also enabled to perform the Vehicle to Grid (V2G) functionality. It monitors electrical parameters and provides data to SMU for voltage and current measurements via Modbus signals. In addition, it interfaces with the AC Low Voltage SCADA that manages the conventional Power Grid, to perform an integral control of a hybrid AC/DC grid.

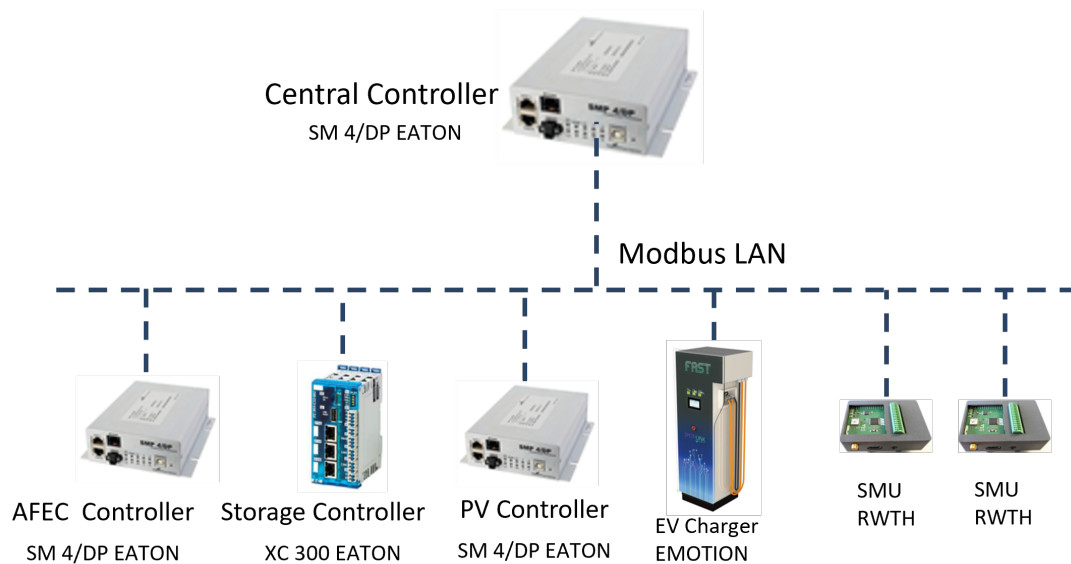


Figure 43: Italian pilot - DC grid local control.

3 Requirements on Test and Validation Services for HYPERRIDE and general DC- and AC/DC Grids

In this Section, a selection of state-of-the-art survey and international test facilities are listed. Specifics on DC testing capabilities related to the HYPERRIDE Project are described and details on laboratory infrastructure, on test setups, and on the testing portfolio are given.

In a recent report (JRC, 2022), a valuable survey and important figures related to smart grid laboratory capabilities have been published. Among many precise information, Chapter 5 "Results: Infrastructure Used and Services Offered" presents novel statistics referring to voltage levels for AC/DC systems of testing infrastructure shown in Figure 44 and Figure 45. Other figures in this report present information related to total power installed, peak power levels, as well as used methodologies such as HIL and real-time simulation for AC/DC systems, respectively.

One of the most important conclusion in this report very few laboratories (3%) according to Figure 45) are capable to offer and conduct DC testing services for voltages higher than 2000 V. This includes both MVDC and HVDC testing and it clearly underlines the urgent need for more testing infrastructure since the demand for respective DC testing is growing.

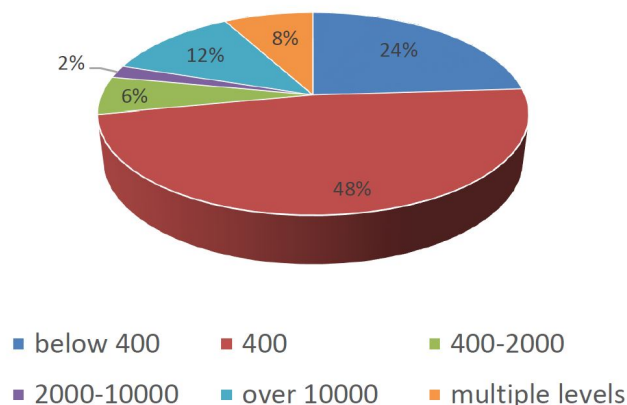


Figure 44: AC voltage level (in V) and the percentage (in %) of labs (source: JRC).

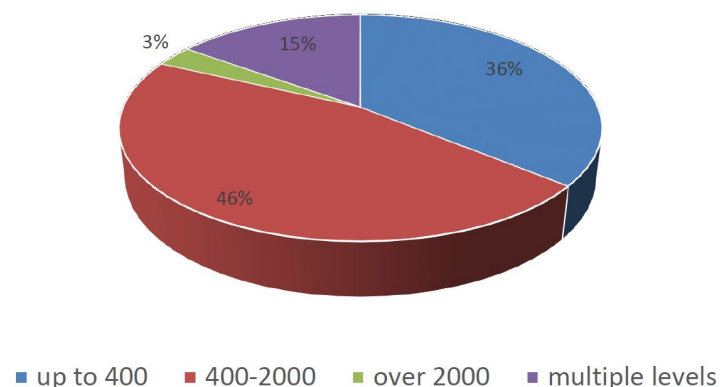


Figure 45: DC voltage level (in V) and the percentage (in %) of labs (source: JRC).

3.1 Fraunhofer IISB, Germany

This laboratory represents a robust, scalable, and innovative test infrastructure for technical devices. It is equipped with a control room for personal and operational safety as well as nearby extensively equipped laboratories to prepare the test devices. The test facility is accessible for trucks up to 40 t and is equipped with a ceiling crane to move loads up to 10 t. Photographic illustrations of the laboratory setup are given in Figure 46 and Figure 47.



Figure 46: IISB MMC test facility (source: Fraunhofer IISB).



Figure 47: Medium voltage test bench at IISB (source: Fraunhofer IISB).

The technical backbone of the facility consists of a public power supply (20 kVac) connection with electrically decoupled via transformers. In addition, a 900 kW water cooling facility and two separate power branches with variable voltage up to 30 kVac via tap-changing transformers and 15 kVdc via 12 pulse rectifier are implemented.

The specific knowledge of this test facility ranges from broad experiences in power electronics development to in-house communication design for software and hardware systems. Close co-operation of IISB are established with FAU Erlangen/Nuemrberg and LZE Bayern. Further advancements are planned with the installation of a motor test bench in the megawatt-scale.

A key topic consists of the Multi Modular Converter (MMC) which is an in-house development from design, planning to testing. Full bridge submodules with explosion-proof housing are designed with 1200 V / 600 A IGBTs and integrated capacitor voltage measurement show various gate driver with safety features. Fiber-optic cable interface for communication and sensor data have been developed as well as the internal power supply from cell capacitor for Field Programmable Gate Array (FPGA) and gate driver. A modular assembly for series and parallel connection is possible and inhomogeneous voltage steps for better power quality can be implemented. The laboratory setup and use cases are shown in Figure 48 and Figure 49.

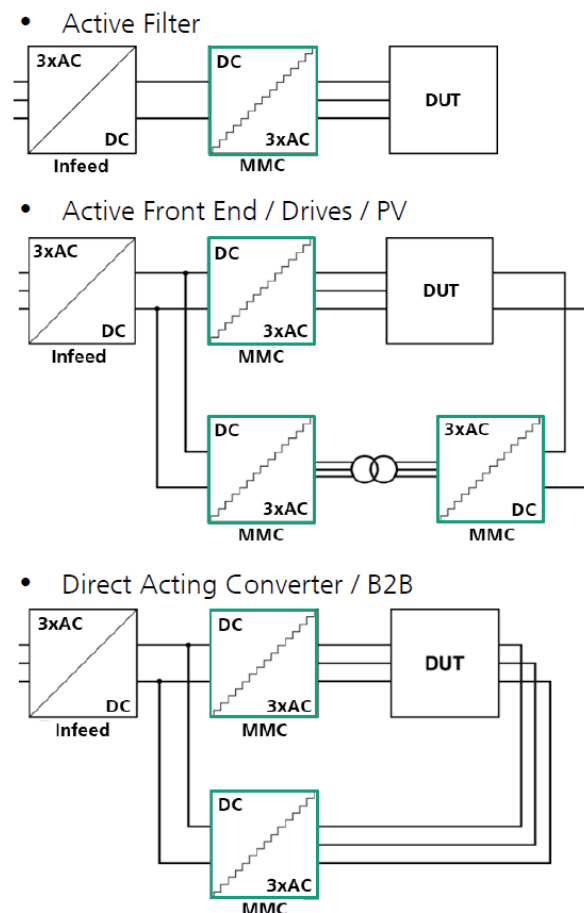


Figure 48: IISB supply connections (source: Fraunhofer IISB).

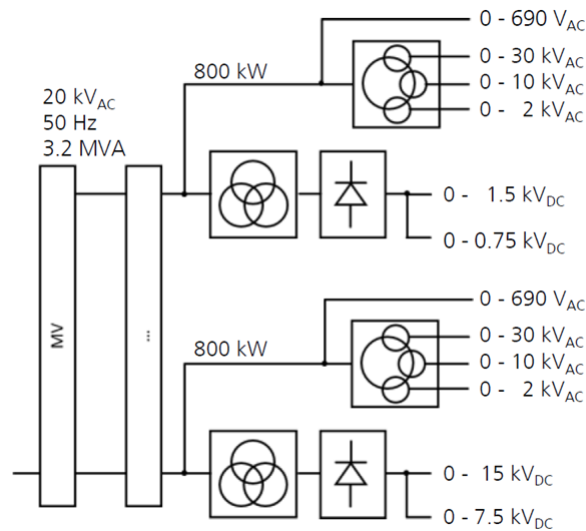


Figure 49: IISB setups (source: Fraunhofer IISB).

3.2 Center of Advanced Power Systems (CAPS), Tallahassee, U.S.

The test facility at Center of Advanced Power Systems (CAPS) is providing several applications related to DC testing such as DC Loading and PHIL (single and multiple PHIL interfaces). In addition, DC load profile and energy storage emulation involves dynamic loading, solar PV emulation, and capacitor and battery banks as well as impedance measurements. As an extension, MMC related applications such as sharing and shifting power among MMC converters at operating levels of up to 10 kVdc and MMC fault behaviour (e.g.: short circuit at terminals) are feasible.

Figures 50 and Figure 51 show block diagrams of DC related test facilities with power amplifiers. The test facility at CAPS is equipped with the following sources and amplification units:

- ABB Direct Current Variable Voltage Source (DC VVS); 0–1.15 kV, 0–2.5 kA, 10 kHz effective switching.
- ABB Modular Multi-level Converter; 4 amplifiers each ± 6 kV, ± 210 A, 12 kHz effective switching; can be arranged to ± 24 kV (series) or ± 800 A (parallel).
- Egston 100 kW, 6-amplifiers; Unipolar: 20–730 V, ± 900 A, Bipolar: ± 710 V, ± 450 A, 125 kHz effective switching.
- TECO Westinghouse DC (and AC) amplifier; 2 power amplifier units (each a 15 kV-class amplifier), 0 – 8.5 kVrms, 0 – 200 Arms, 84 kHz effective switching (168 kHz with two units in series), Configurable AC: 0-17 kVrms, 0-200 Arms, (2 units in series), 0 - 1.2 kVrms, 2.8 kArms and DC : 0 – ± 28 kV, 0 \pm 200 A or 0 – ± 1.2 kV, 0 - ± 4 kA.
- DRS Compact AC/DC amplifier; 0 - 1 kV, 0 - ± 1 kA.

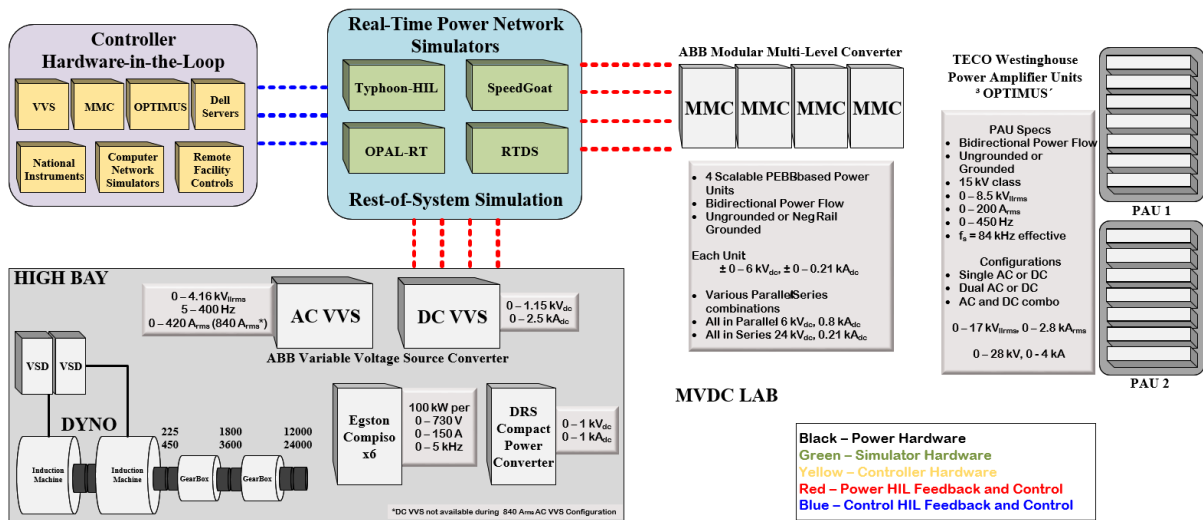


Figure 50: HIL facility overview at CAPS (source: CAPS).

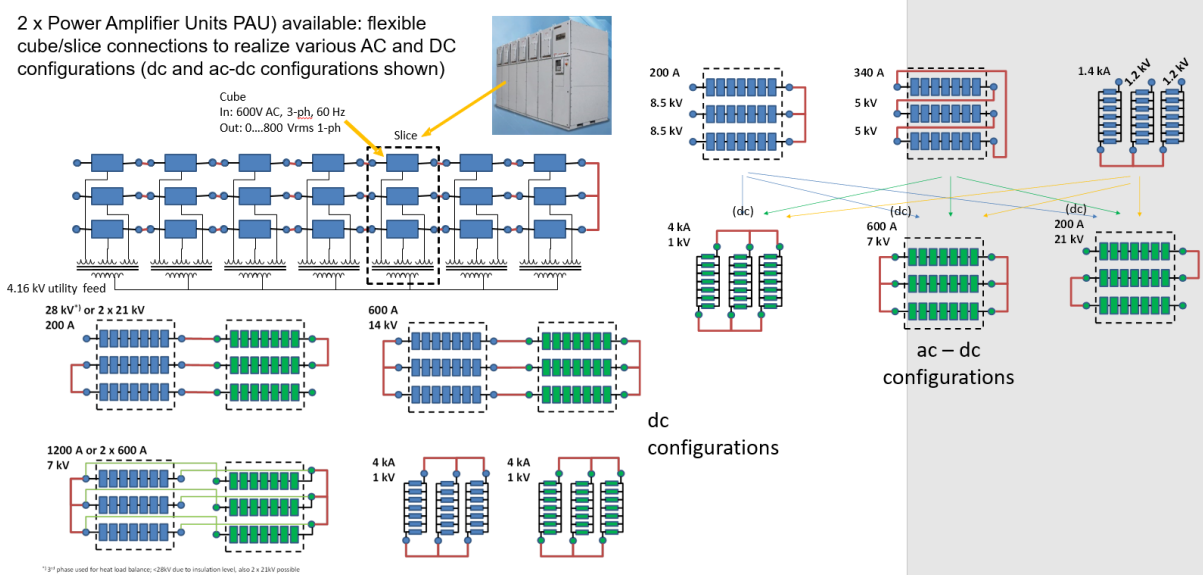


Figure 51: Reconfigurable MW-class PHIL amplifier (source: CAPS).

3.3 Hydro-Québec's research institute (IREQ), Varennes, Canada

The power system simulation and distribution test line facilities is located in Varennes Campus, Canada and the owner is Hydro-Québec. Numerous large-scale real-time power system simulators enable tests of full scale control system replicas for PHIL/CHIL tests such as static VAR compensators, Static Synchronous Compensator (STATCOM), High Voltage Direct Current (HVDC), synchronous condenser, Battery Energy Storage System (BESS), microgrid, PV inverters, or grid automatization/protection. MW-scale PV power plants and battery energy storage are available for testing purposes and a 25 kV (overhead and underground) distribution test line exists that includes energy storage, diesel generators, loads and microgrid controller.

The power system simulation lab setup depicted in Figure 52 shows the following application ranges: Development of simulation software packages (Hypersim, EMTP-RV, Simscape Electrical) and model libraries (generic control systems, wind generators, Distributed Energy Resource (DER)s . . .). In addition, the realization of real-time studies of complex, real-time power systems as well as the testing of control and protection, commissioning of interconnections, operating strategies, performance and settings optimization, and the validation of new concepts is performed. Based on this concept, interactions between series-compensated networks, real HVDC controls, and large-scale wind power plants are studied. The simulation lab consists of following installation:

- 51 x Hypersim real-time simulators: 7 x HPE/SGL (728 calculation cores), 13 x OPAL-RT (200 calculation cores), 31 x RTPC (388 calculation cores).
- 1 x Speedgoat and 1 x Typhoon HIL real-time simulators.
- 15 x transmission system CHIL test areas.
- PV array simulator: 1500 V, 15 kW; 5 x 1-5 kW residential PV inverters.
- High bandwidth closed-loop PHIL grid simulator: 0 to 208 V 3-phase AC, 3 kVA.
- Digital substation test setup and co-simulation platform.

In parallel to the simulation laboratory, Hydro Québec operates a distribution test line laboratory shown in Figure 53 for testing of advanced distribution devices, new protection schemes, remote microgrid testing, and interoperability testing. The emulation of different load characteristics, including real and reactive power, power factor, voltage dependency, and harmonics can be investigated.

The integration of DER with smart distribution applications represents a test area (SIMP Power Simulator) to develop and validate green technologies for efficient generation, delivery and end-use of electricity. Microgrid controller testing and validation with a high penetration of renewable generation is assessed with the help of this setup shown in Figure 54 which consists of following installations:

- 25 kV overhead and underground distribution line.
- Short-circuit reactor (5 kA / 14 kA asymmetrical).
- Grid line impedance emulator (2 x 60 km equivalent).
- Shunt capacitors (2 x 1.2 Mvar).
- Battery energy storage (EVLO 1 MW / 2 MWh), Diesel generators (400 kVA, 1063 kVA).
- Induction motor (200 Hp), Solar power plant (1.5 MW).



Figure 52: Real-time power system simulator lab at IREQ (source: Hydro-Québec).



Figure 53: Full-scale distribution test line test setup at IREQ (source: Hydro-Québec).

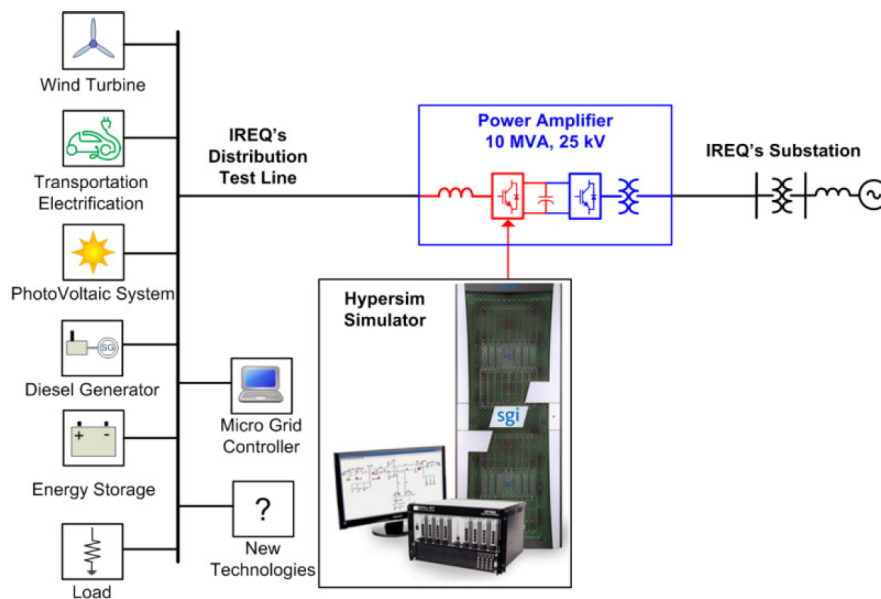


Figure 54: SIMP power simulator at IREQ (source: Hydro-Québec).

3.4 Existing Standards and Normative Frameworks

Definition of test- and validation infrastructure/procedures for concrete HYPERRIDE solutions for preparing demonstrations and general requirements for hybrid AC/DC grids including actual standards and normative frameworks. The following tables and lists should support the reader to get an overview which national and international standards are existing and in which areas and for which application standardisation shows an incomplete status or is missing.

In Table 9 and Table 10, a relevant set of required Low Voltage Direct Current (LVDC) and Medium Voltage Direct Current (MVDC) component and system solutions (to be extended) from Deliverable D2.3 Chapter 10 can be found.

In Table 11, detailed descriptions and related standards of DC components and respective system testing can be found according to (Jambrich et al., 2020). Here, DC applications and systems specifically designed for LVDC and MVDC are highlighted. It is notable that not for all DC applications are covered by existing standards. However, the methodology of real-time based HIL testing may be used for a wide spectrum of applications.

Table 12 shows available LVDC standards as listed according to (Smith, Wang, Emhemed, Galloway, & Burt, 2018). This list involves standards specifically valid for the United Kingdom (UK), however, references to international IEC standards are given as well. From this list it becomes obvious that norms and standards are missing for certain DC applications. In future it will be necessary to demonstrate an equivalent or higher level of safety compared to AC systems in order to prove cost and environmental benefits of LVDC applications. In particular, further normative efforts are required in the area of fire prevention from DC-arcs, in general.

Table 9: Relevant set of required LVDC component and system solutions.

LVDC Component	Demo in WP (6-8)	Technical Issues (1-8)	Specs in WP (3-8)
Power converters	6, 7, 8	1-8	3, 6, 7, 8
Fuses	tbd.	1, 2, 7, 8	6-8
Arresters	tbd.	1, 2, 7, 8	6-8
Harmonic-Filters (AC-side)	6, 7, 8	1, 2, 3	6-8
Grounding equipment	6, 7, 8	1, 2, 3	6-8
Switching devices (disconnectors, breakers, residual current devices)	6, 7, 8	1, 2, 7, 8	3, 6, 7, 8
Power cables and accessories	6, 7, 8	1, 7, 8	6-8
Switchyard/compartments	6, 7, 8	1-8	6-8
Sensors, DC-MUs, meters	6, 7, 8	1-8	3
Secondary (control, protection relays, ICT)	6, 7, 8	1-8	3, 4, 5
Generation (photovoltaic plant)	6, 7, 8	1-8	6-8
Storage (battery, supercapacitor)	6, 7, 8	1-8	6-8
Loads (EV charging)	6, 7, 8	1-8	6-8
Grid planning and simulation	6, 7, 8	1-4, 6-8	4
AC/DC product test and validation	6, 7, 8	1-8	3
Mitigation of faults and cascade effects	6, 7, 8	1, 2, 4-8	5
Cyber security, thread detection	6, 7, 8	1, 2, 4-8	5

Table 10: Relevant set of required MVDC component and system solutions.

MVDC Component	Demo in WP (6-8)	Technical Issues (1-8)	Specs in WP (3-8)
Power converters	6, 7	1-8	3
Fuses	tbd.	1, 2, 7, 8	6-8
Arresters	tbd.	1, 2, 7, 8	6-8
Harmonic-Filters (AC-side)	6, 7	1, 2, 3	6, 7
Grounding equipment	6, 7	1, 2, 3	6, 7
Switching devices (disconnectors, breakers, residual current devices)	6, 7, 8	1, 2, 7, 8	3
Power cables and accessories	6, 7	1, 7, 8	6, 7
Switchyard/compartments	6, 7	1-8	6, 7
Sensors, DC-MUs, meters	6, 7	1-8	3
Secondary (control, protection relays, ICT)	6, 7	1-8	3, 4, 5
Generation (photovoltaic plant)	6, 7	1-8	6, 7
Storage (battery, supercapacitor)	6, 7	1-8	6, 7
Loads (EV charging)	6, 7	1-8	6, 7
Grid planning and simulation	6, 7	1-4, 6-8	4
AC/DC product test and validation	6, 7	1-8	3
Mitigation of faults and cascade effects	6, 7	1, 2, 4-8	5
Cyber security, thread detection	6, 7	1, 2, 4-8	5

Table 11: Overview over DC components and DC systems testing.

		Topics	Methods
Components	Power cables	DC nominal voltage, electric strength of insulation, inversion of field, space-charge debunching, temperature and polarity reversal behaviour	MV: pre-qualification VPE-cables CIGRE TB 496 (HVDC) load cycles with voltage and current load (temperature rise test), polarity reversal, testing voltages (IEC-standards)
	Fuses	Electric impedance, rated and testing current, thermal test, switch off capacity, switching characteristics	LV fuses (PV): IEC 60269-6 HH-fuses: – (IEC 60282).
	Surge arrester	Voltage test, safety level, insulation resistance, air gap and creepage distances, dielectric resistance, short-circuit current capability	LV (PV): EN 50539-11,-12,-32, IEC 61643-31,-32 LV (Wind): DIN CLC/TS 50539-22MV: IEC 60099-9
	Switching devices (disconnecter and circuit breaker, residual current operated device, ect.)	Switching: missing current zero crossings with DC (electric arc), high system dynamics at short-circuit events, mechanical functionality tests, electric and mechanic endurance test, thermal and insulation test, short-circuit and load shedding tests, short-time current behaviour, tripping characteristics, ect.	LV: residual current operated device: IEC 61008 (AC+DC); IEC 61009 (DC) circuit breaker: IEC 60898-2,-3 circuit breaker: IEC 60947-2; Annex P load-break switch: IEC 60947-3; Annex D, train applications up to 3kVdc: EN 50123-4
	Switching equipment	Isolation: power cables (insulation materials, ect.), electric and mechanic endurance test, short-circuit and load shedding test, short-time current behaviour, ect.	Train applications up to 3kVdc: EN 50123-1,-6, IEC 61992
	Transducers, meters, IEDs, sensors (incl. electric arc detection)	Insulation strength, accuracy, electric arc and temperature reliability, thermal durability, frequency behaviour, power quality, calibration, functionality, communication	Transducers: IEC 61689-1,-6,-14,-15 meters: IEC 62053-1,-41
	Converters, solid insulation electric transformers, ect.	Grid integration, safe operation, functionality	C/PHIL, train systems: EN 50328, IEC 62590, IEC 60700-1,-2
	AC-coupling incl. active, bidirectional rectifier	Grid integration, safe operation, functionality	C/PHIL; LV: IEC 62909-1,-2 (PV and storage), EN 62093, EN 62109, EN 62920 (PV) MVDC: IEC 62477-1,-2
	Auxiliaries (control, communication)	functionality, safe operation	Protective relay (IEC 60255-1)
Installations	Generation	Grid integration, safe operation, automation	PHIL, IEC TS 61936-2, IEC 60364-1,-7-712 (PV), ÖVE E 8101
	Storage	Grid integration, safe operation, automation	PHIL, IEC TS 61936-2, IEC 60364-1, ÖVE E 8101, IEC 62619 (Li-Ion)
	Loads (incl. electric mobility)	Grid integration, safe operation, automation	PHIL, IEC TS 61936-2, IEC 60364-1, ÖVE E 8101, IEC 61851, IEC 62196
Systems	Point of common coupling	Safe operation, automation, functionality	PHIL (e.g. residential areas with DC bus)
	Micro grids	Grid automation (energy management, safe operation)	PHIL (e.g. local energy communities)
	Distribution grids	Grid automation (load flow management, safe operation)	PHIL (e.g. grid operators incl. LV/MV coupling)
	AC/DC hybrid grids	Grid automation (load flow management, safe operation)	PHIL (incl. AC coupling)

Table 12: Available LVDC standards

	<i>Application</i>	<i>Protection criteria</i>	<i>Safety</i>	<i>Power quality</i>	<i>Earthing & Bonding</i>
LEVEL 1: <120 V	USB	USB-IF (2.0, 3.0, Type-C) BS EN 62680-2-1	USB-IF (2.0, 3.0, Type-C) BS EN 62680-2-1	USB-IF (2.0, 3.0, Type-C) BS EN 62680-2-1	USB-IF (2.0, 3.0, Type-C) BS EN 62680-2-1
	Telecom (48V)	ETSI EN 300 132-2TR 100 283	ETSI EN 300 132-2	ETSI EN 300 132-2	ETSI EN 301 605
	LED Lighting	BS EN 61347 2-13 BS EN 61347-1	IEC 60598-1 IEC 61347-1	BS EN 62384	IEC 61347-1
	PoE	NEC.725	-	IEEE 802.3at	-
	Residential	-	BS7671 NEC	-	BS7671 NEC
	Building	-	BS7671 NEC	-	BS7671 NEC.250
LEVEL 2: 120-400 V	Telecom (120 - 400V)	ETSI 300 132-3-1 ITU-TL.12(00-05)	ITU-TL.12(00-05)	ETSI 300 132-3-1 YD/T2378-2011 YD/T2089-2016	ETSI EN 301 605 ITU-TL.12(00-05)
	EV Charging	BS EN 61851-23:2014	BS EN 61851-23:2014	BS EN 61851-23:2014	-
	Data Centre	BS EN 50600-2-2:2014	BS EN 50600-2-2:2014 IEC62040-5-1	BS EN 50600-2-2:2014	ETSI EN 301 605
	Traction	BS EN 50123-7-1 BS EN 50123-1	BS EN 50328 BS EN 50633	BS EN 50328 BS EN 50163	IEC 62128 IEC 60364-4-41
LEVEL 3: 400-1500 V	Public Networks	-	P2030.10 NEC.712	-	NEC.250
	Ship Power	IEC 60092-507 ABYC E11	IEC 60092-507	IEC 60092-101	-
	Solar PV	BS EN 60269-6 BS EN 62548-1	BS EN 62109-1 IEC 60364-4-41	BS EN 62109-1	IEC 60364-7-712

4 DC-Arc Fault Testing.

First DC-arc experiments were done with AIT's new DC-cube, which was already introduced in Section 2.1.2. In general, in DC-grids two types of arc faults can be distinguished:

- (i) High power arc faults: the source of power comes from batteries, capacitor banks or rectified transformer sources (incl. fail operation of current limiting elements like fuses, circuit breakers, semiconductors, etc.)
- (ii) Low power arcs: arc typical in series with a current limiting element like an electrical load (resistor) or power-regulated current source

This leads to different kinds of possible danger and risks: Ad (i): large short-circuit currents leading to large hazardous explosions: hot gas exhausts dangerous for human, pressure waves and bulk pressurisation dangerous for enclosures and buildings, the arc is terminated by a fuse or circuit breaker in 5 - 250 ms. Ad (ii): undetected arcs, long burning times, leading to damages of equipment, scenario (i) or to fires. The effect of big hazardous DC-arc-explosion was already in the focus of the Deliverable D3.3.

The aim of this section is to investigate the differences of the behaviour of DC- and AC-arcing in the medium power class of approximately 1 MW. Figure 55a shows the enclosure used for DC-arc testings and the positions of the pressure sensors p9 (central) and p10 (upper). Figure 55b shows the adjustable gap between busbars and the ignition wire.

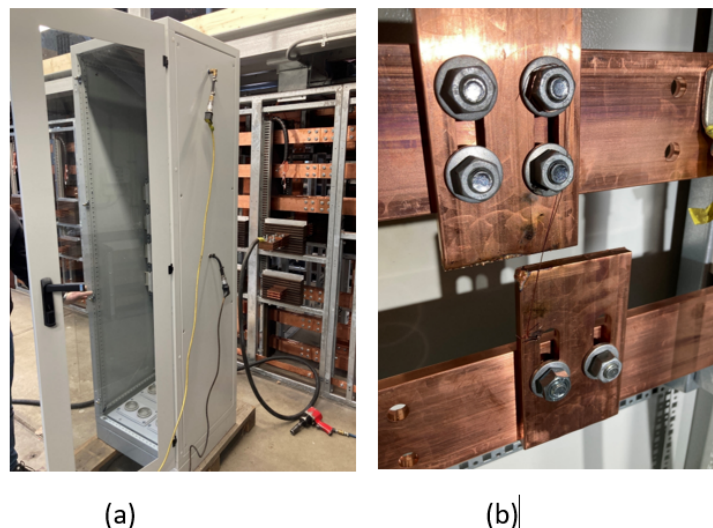


Figure 55: (a) Enclosure used for DC-arc-testings (b) adjustable gap between busbars incl. ignition wire.

Figure 56 shows the DC-arcing emitting intensive radiation in the visible and UV-range and the plasma jets in the middle (brighter). The DC-arcs are highly mobile and can over-span a large distance between electrodes.

Figure 57 shows the movement of the arc from its point of ignition to the left border within 10 ms. The arc current is connected to a magnetic field whose effect on the charge carriers (electrons and ions) is a force directed towards the arc axis. In arcs with contracted electrode areas at the base points, the current density and thus the pressure decreases from the electrodes towards the arc column, i.e. there is a pressure gradient in the axial direction, which results in a plasma flow directed away from the electrodes. This leads to the formation of club-shaped cathode and anode beams that are almost perpendicular to the electrode surface.

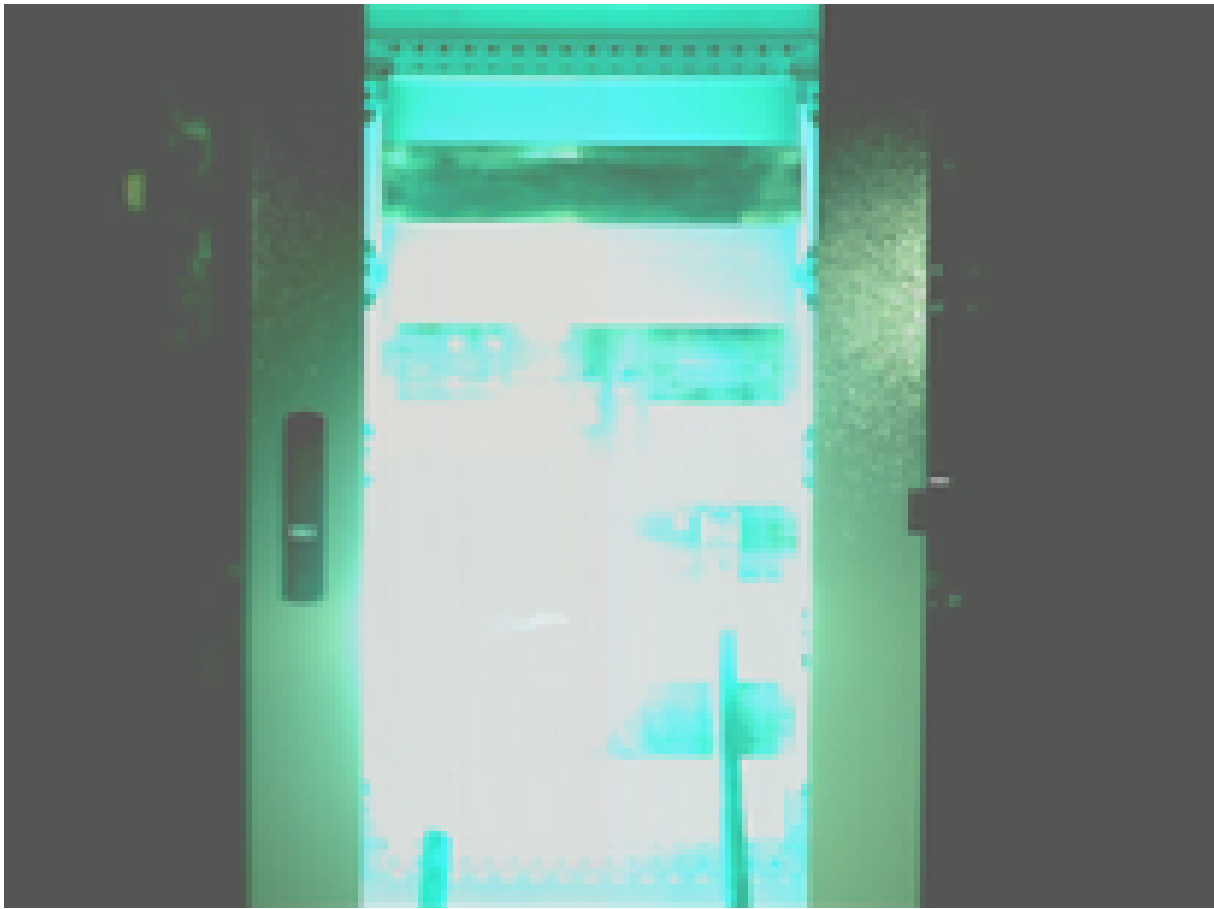


Figure 56: DC-arc in the enclosure (without dark filter).

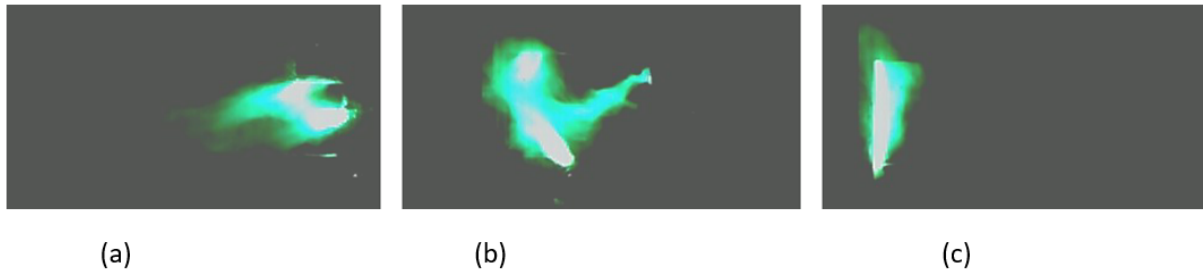


Figure 57: Time-Sequence using a dark optical filter showing the movement of the arc from left to right.

In Figure 58, oscillograph curves of current, voltage, pressure (p9), pressure (p10), and power (P) are presented. The pressures p9 and p10 show a peak value (of rms-data) of 6 mbar and 40 mbar, respectively. An FFT (Fast Fourier Transform) of p9 and p10 signals give the typical 2.1 kHz-peak which is caused by acoustic standing waves. The arc-voltage shows a noisy time-dependence, which is typical for arcing-processes. Both signals in combination with a current-measurement system and optical detection can be used for the development of future DC-arc fault mitigation systems. The current shows the typical ripples of a B12 rectifier. Spikes in the current curve are not true. They are caused by induction in the commutation points and can be ignored.

In comparison to AC, due to the lack of current zero crossings, the DC-arc can build up a higher voltage and can bridge longer distances. The experiment has shown that the DC-arc can exist also at an electrode-distance of 7 cm with an relatively moderate current of approximately 2 kA. It is notable that this behaviour is in strong contrast to typical characteristics of AC-arcs.

Summarising the arc-fault-risk considerations, the power turn over of potential DC-arcs can be estimated by measuring the spacing between the bus bars. Due to probable arc-runs, the largest bar spacing should be taken inside or outside the enclosure (the arc can be also blown out of the enclosure). If the open-circuit voltage is less than the arc voltage, the arc cannot longer exist and extinguish. The arc voltage U can be calculated by $U/d = 30 \text{ V/cm}$, where d is distance between the electrodes. With this arc-voltage the available current has to be calculated by a circuit simulation program. As an overestimation on the secure side also the short-circuit-current of the grid can be used. The energy turn over of the DC-arc can then be calculated by multiplying the power of the arc by the switch-off-time given by the semiconductor circuit breaker or fuse.

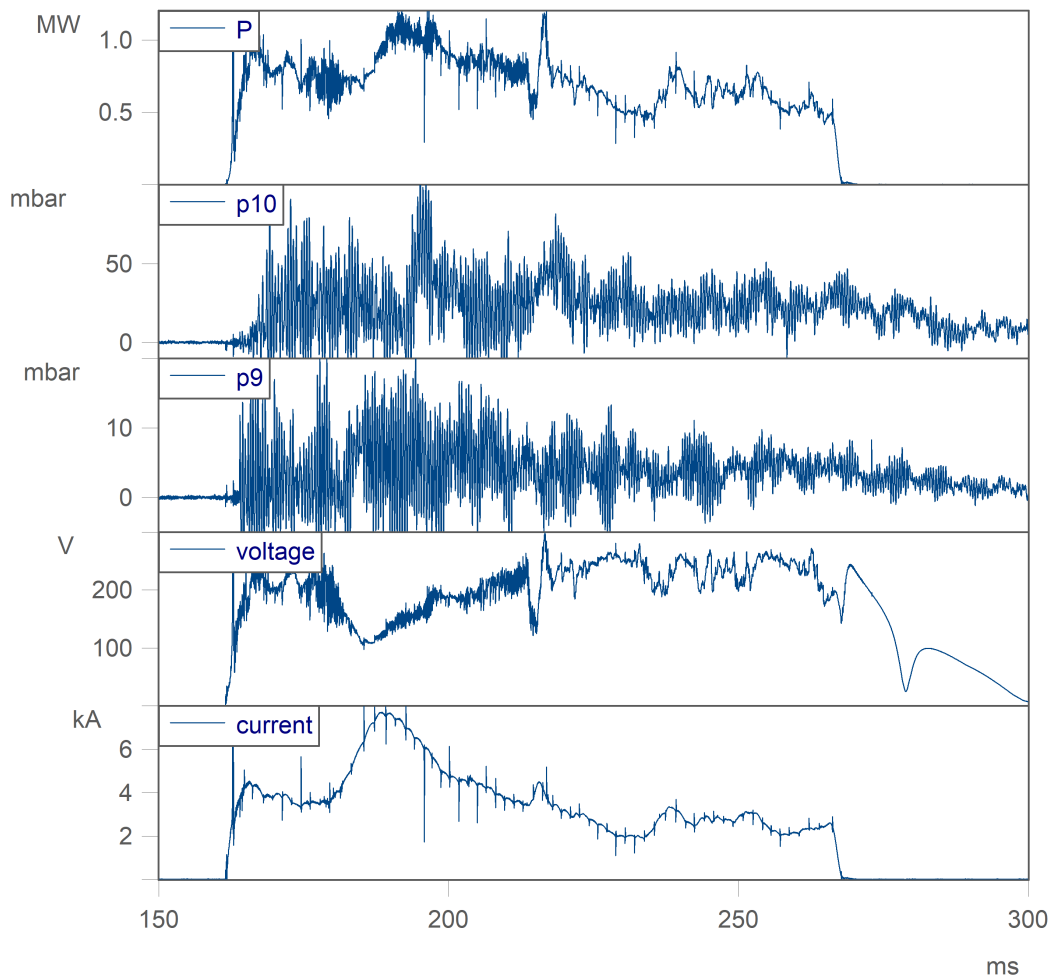


Figure 58: Oscillograph curves of current, voltage, pressure (p9), pressure (p10) and power (P).

5 Conclusions

In this Deliverable, major testing facilities referring to LVDC, MVDC, and HVDC laboratory setups are presented in detail. In what follows, major conclusions are highlighted and referred to the works within the HYPERRIDE project.

As a first conclusion, it can be stated that for LVDC testing building blocks and laboratory infrastructure is existent, nowadays. For MVDC, a lot of planning to extend the technical infrastructure is missing in order to be able to meet the technical demand and future testing requirements of industry (Makkieh et al., 2021), (Ma et al., 2020).

As a second conclusion, it can be assessed that the European Union focuses on Strategic Energy Technologies (SET Plan). The existing “implementation working group” on high-voltage DC will widen its focus to include low-voltage DC with the new name “SET Plan Implementation working group DC”. The group report includes chapters on regulation and specifically in sections related to priorities and targets.

As a further conclusion, test laboratories have to be equipped to conduct component and system testing for DC with respect to the integration of existing 10/20/30 kVac voltage levels. For this purpose, existent standards have to be adopted and reworked with respect to insulation strength, system dynamics, ect. Actual prototypes of fully solid-state DC circuit breakers and hybrid DC circuit breaker show operation times in the range of 1-50 μ s and of 0.3-2 ms, respectively (standard electromechanical: 5-8 ms for fault clearing), and the resulting impact, e.g. (short-circuit) current peaks on system dynamics of power converters/electric capacitors dominated DC grids is not yet covered in existent normative frameworks for AC- and DC grids as reports show (T. IEC, 2020).

As an outlook and discussing further works, the following items are discussed with respect to works of this Deliverable within the HYPERRIDE-project.

It is notable that many national activities such as pilots or testing and research infrastructure are currently established or are in the planning in South-Korea and in the P.R. China. These efforts are covering all DC voltage levels of LV-, MV-, and HVDC for the purpose of grid integration. For future research, collaborations and synergies with respective Asian research facilities should be established for moving further towards harmonising efforts and know-how exchange.

In future, intentions for the harmonisation of existing guidelines can be observed. Namely, guidelines for LVDC system concepts of the DC industry Open DC Alliance and concepts focused on building infrastructure CurrentOS Foundation should be harmonised on an IEC level. For this ongoing works, further important standardisation efforts such as SyC LVDC (IEC, 2024) or for MVDC class CIGRE TB 875 (CIGRE, 2022) or CIGRE TB 931 (CIGRE, 2024) have to be taken under consideration.

It is crucial for further applications and increased usage of DC system components in existing grids that not only laboratory testing but also training centers have to be installed in Europe in order to create attraction for stakeholders. As an initial step, one HYPERRIDE partner, the FEN partner in Aachen, is trying to establish such a training facility to create awareness of the DC topic.

References

- CIGRE. (2022). Medium voltage dc distribution systems. *Technical brochure TB875, CIGRE*.
- CIGRE. (2024). Technical requirements and field experiences with mv dc switching equipment. *Technical brochure TB931, CIGRE*.
- Holzbauer, M. (2023). *Development of a closed-loop hall sensor for high current measurements in mvdc grids* (Unpublished master's thesis). University of Applied Sciences Wiener Neustadt.
- IEC. (2024). Low voltage direct current and low voltage direct current for electricity access. IEC. Retrieved from <https://www.iec.ch/energies/lvdc>
- IEC, T. (2020). Iec tr 63282; lvdc systems—assessment of standard voltages and power quality requirements. *IEC: Genève, Switzerland*.
- Jambrich, G., & Fuchs, N. (2021). Cired wg 2019-1 dc distribution networks-final report. *DC DISTRIBUTION NETWORKS-WG 2019-1*.
- Jambrich, G., Lehfuss, F., Stöckl, J., Mayr, J., Ledinger, S., & Kupzog, F. (2020). Entwicklung von p-hil-testmethoden und forschungsinfrastruktur für mittelund niederspannungs-dc-systeme. *Elektronik & Informationstechnik (e&i)*, 406–414.
- JRC. (2022). Jrc science for policy report, smart grid laboratories inventory.
- Ma, Z., Li, R., Lürkens, P., Han, M., Kim, S., et al. (2020). Medium voltage direct current (mvdc) grid feasibility study. *Technical brochure TB793, CIGRE*.
- Makkieh, A., Burt, G., Alzola, R. P., Jambrich, G., Fuchs, N., Kazerooni, A., . . . others (2021). Dc networks on the distribution level—new trend or vision?
- Smith, K., Wang, D., Emhemed, A., Galloway, S., & Burt, G. (2018). Overview paper on: low voltage direct current (lvdc) distribution system standards. *International Journal of Power Electronics*, 9(3), 287–310.

Consortium



Disclaimer

All information provided reflects the status of the HYPERRIDE project at the time of writing and may be subject to change.

Neither the HYPERRIDE Consortium as a whole, nor any single party within the HYPERRIDE Consortium warrant that the information contained in this document is capable of use, nor that the use of such information is free from risk. Neither the HYPERRIDE Consortium as a whole, nor any single party within the HYPERRIDE Consortium accepts any liability for loss or damage suffered by any person using the information.

This document does not represent the opinion of the European Community, and the European Community is not responsible for any use that might be made of its content.

Copyright Notice

© 2024 by the authors, the HYPERRIDE Consortium. This work is licensed under a "CC BY 4.0" license.

